ORIGINAL PAPER

Soil erosion and flood hazard zonation using morphometric and morphotectonic parameters in Upper Alaknanda river basin

Neeraj Pant[1] · Rajendra Kumar Dubey[1] · Anand Bhatt[2] · Shive Prakash Rai[3] · Prabhat Semwal[2] · Sumit Mishra[2]

Abstract

In the present study, detailed morphometric, morphotectonic, statistical and hazard analyses have been carried out in the Upper Alaknanda river basin (UAB) located in Central Himalayas, Garhwal, India. The study area is bounded by the South Tibetan Detachment System in the north and by the Main Central Thrust in the south. The major river flowing in the area is Alaknanda which is a major tributary of river Ganga. The purpose of this study is to examine the influence of active tectonics, flood hazard, and soil erosion on the basis of morphotectonic and morphometric parameters using the Cartosat-1 Digital Elevation Model and ArcGIS software. The study area is divided into 10 sub-basins, where 50 morphometric and 6 morphotectonic parameters were calculated. Bifurcation ratio and stream frequency show that streams up to third order is having steep gradient and rolling through highly dichotomized terrain, due to which high overland flow and less groundwater recharge takes places, whereas drainage density clearly indicates the high flood possibility in the region. Morphotectonic parameters indicate relatively young to an early mature geological stage of sub-basins and tectonically active region. The statistical analysis of morphometric parameters is carried out by using correlation analysis, hierarchal cluster analysis, and principal component analysis. Based on their susceptibility to soil erosion, morphometry and landcover classification is carried out to prioritize the sub-basins of UAB. The combined morphometric, morphotectonic and statistical analysis indicates that the area is tectonically active and highly prone to flood, flood induced landslide and soil erosion. The case study of the 2013 flash flood event at three locations Benakuli, JP HEP and Pulna also confirms that the study area is hydro-geologically active to flood and flood induced hazards. The results obtained in this study are directly related to watershed management and hence soil erosion, tectonic activities and flash flood possibilities should be taken into consideration during future development in the area.

Keywords Upper Alaknanda river basin (UAB) · Central Himalaya · Morphometry · Morphotectonic · Hierarchal cluster analysis · Watershed management

✉ Rajendra Kumar Dubey
rkdubey1085@hotmail.com

Extended author information available on the last page of the article

1 Introduction

The snow and glacier dominated Himalayan province of India are hydrologically significant sources of freshwater resources. The sustainability of these water resources depends upon the climatic and geological or geomorphological conditions of the regions. The Himalayan Mountain Ranges are unstable due to tectonic activities and seismically active zones (Valdiya 1999a, b). After the upliftment of Himalaya, great distortion, and structures were developed due to tectonic activities in past, which is growing till now due to neo-tectonic activities (Nag and Chakraborty 2003; Pérez-Peña et al. 2010; Demoulin 2011). Due to these tectonic and non-tectonic activities, even firm and competent rocks become fractured and brittle that finally leads to various kinds of mass movements and geomorphological changes which are also supported by other epigenetic forces like rain, avalanches, freezing and thawing actions (Valdiya 1999b; Bali et al. 2012). These factors are responsible to increase river opening, drainage basin irregularity, river alteration and hence has a substantial impact on the drainage network behaviour or the hydrology of the area (Pérez-Peña et al. 2010; Walker and Allen 2012; Sajadi et al. 2019). To understand and investigate the deformational process caused by active faults and regional tectonic activity, drainage networks system are the key factors (Lin et al. 2009; Yan and Lin 2015). The drainage feature of a basin depends on its runoff and infiltration capacity, which specifically acts as measures of soil erosion intensity and has been defined as an important criterion for erosion risk assessment (Sharma et al. 1985).

Morphometric and morphotectonic analysis technique have played a significant role to understand the hydrology of these drainage basins (Strahler 1952a, b; Bishop 2002; Ritter et al. 2002). Morphometric analysis helps to understand the basin dynamics, morphological changes, temporal physical changes and its effect over anthropogenic activity or natural disturbances in drainage system of a basin (Thompson et al. 2001). It also provides a linkage between different land surface processes and land system components such as geomorphology, hydrogeology and landcover (LC) (Astras and Soulankellis 1992; Ifabiyi et al. 2012). Morphometric studies were introduced by Horton (1940) and Strahler (1950), the idea was further developed and improved by many authors like Miller (1953), Schumm (1956), Melton (1958), Morisawa (1962) and Clarke (1966). The morphometry is the mathematical analysis of the surface, structure and proportions of the earth's landform configuration (Clarke 1966). It helps to identify the zones which are susceptible to natural hazards basically controlled by the action of water like flood, mass movements, tectonic activities and soil erosion (Patton and Baker 1976; Diakakis 2011; Romshoo et al. 2012; Wakode et al. 2013). Hence, these kinds of studies are significant for the sustainable development of any watershed management program.

The field-based survey and investigations are limited in the higher Himalayan regions, due to adverse geographical and topographic conditions. Therefore, remote sensing and GIS techniques play an important role in providing a suitable solution and better understanding of the hydrological processes in regional scale on the Himalayas. These days the remote sensing and GIS is an important and powerful technique or tools which integrates special and non-special information from the various sources to understand catchment and its morphometric parameters with detailed investigations and for decision making (Williams et al. 1972; Mesa 2006; Lyew-Ayee et al. 2007; Bali et al. 2012; Shukla et al. 2014; Maeda et al. 2014).

The present study area falls under the head water region of the Upper Alaknanda river Basin (UAB), Central Himalayas, India. The Alaknanda river originates from the snout

(3800 m asl) of Satopanth glacier. It flows through Hindu pilgrimage center 'Badrinath' and meets to Bhagirathi river at Devprayag covering ~ 200 km in the basin and after the confluence, it is named as Ganga River. Overall, the hydrological response of Alaknanda river has a major impact over Ganga river, which affect million people living in the basin and at the downstream of the basin. There are few studies that have been carried out in Alaknanda river basin with the help of morphometric or morphotectonic analysis (Bali et al. 2012; Shukla et al. 2014; Rana et al. 2016; Anand and Pradhan 2019). These studies mainly deal with the whole Alaknanda river basin or for lower Alaknanda river basins. In this present study, we have tried to recognize the role of morphometric and morphotectonic parameters along with various statistical analysis, for integrated basin management for the head water region or Upper Alaknanda river basin (UAB) (from Satopanth and Saraswati basin to Vishnuprayag) in Central Himalayas of India. Various multivariate statistical analysis (Correlation coefficient analysis, cluster analysis and factor analysis) has been used to transform and organize the data sets into small groups which characterizes the similar evidence from the original data set. We have also done a case study of three different locations where the major flood event occurred in 2013 to highlight the effects of flash flood in UAB basin. The main objectives of the study are; to (i) analyse the morphometric and morphotectonic parameters to understand the hydrology of the Upper Alaknanda river basin (ii) prioritisation of the sub-basins on the basis of morphometric and morphotectonic characteristics (iii) identification of zones susceptible to high soil erosion and tectonic activities.

2 Study area

2.1 General

The study area is located between 30.504888°N–31.045426°N latitude and 79.607289°E–79.373762°E longitude of Garhwal Himalaya and covering a basin area of ~ 1527 km² with a main channel length of 71.5 km (Fig. 1). The area is represented by Higher Himalaya and range from 1411 m to 7136 m asl in elevation. The Alaknanda is the major river of the study area which originates from the snout (3800 m asl) of Satopanth glacier and is known as the major tributary of River Ganga (Fig. 1). Alaknanda river system drains through three districts Chamoli, Tehri and Pauri of Uttarakhand and contributes about 68–74% of total discharge in river Ganga at Devprayag (Singh and Hasnain 1998). During summer months, flow of the river is mainly sustained by snow and glacier melt when the demands of water, for drinking, irrigation and hydropower generation is at peak. Three important hydropower projects, namely Lata-Tapovan (170 MW capacity), Tapovan-Vishnugarh (520 MW capacity) and Vishnugarh-Pipalkoti (440 MW capacity) are either in operational or constructional phase in the Alaknanda river basin. Alaknanda catchment is also famous for Hindu mythological temples which attracts thousands of tourists every year during summer months. Overall, the hydrological response of Alaknanda river have major impact over Ganga river, which affect millions of people living in the basin and at the downstream of the basin.

The climate of the study area is subtropical to alpine type with the average annual rainfall ranging from 600 to 1200 mm (Joshi and Kumar 2006). The maximum temperature in the area increases up to 35 °C in June and reduces the minimum up to as low as − 17 °C in January, respectively. The study area consists of high mountain ranges in the northern part (in north-western and north-eastern) that are mostly covered with snow and glaciers
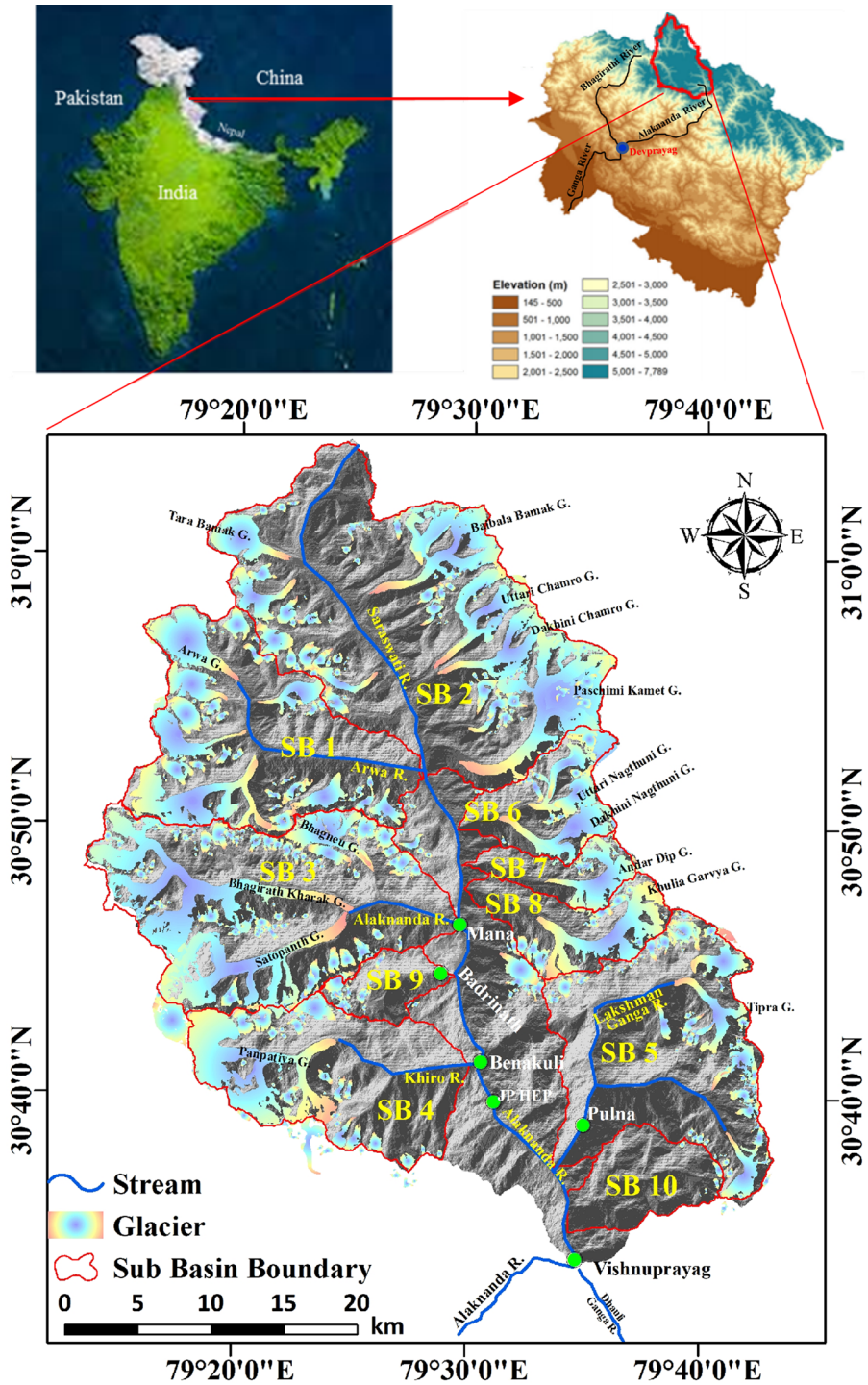
Fig. 1 Study area map of Upper Alaknanda river basin with its location in the country and in Uttarakhand

all over the year. Geomorphologically UAB has diverse physiography that includes hills, Glacial valley systems, U and V-shaped valleys, terraces piedmont zones, etc. It consists of major river, known as Alaknanda river and have many other tributaries like Saraswati, Khiro Ganga, Lakshman ganga and Dholiganga. All the major rivers in the Alaknanda Basin are perineal, as both rainfall and glacial/snow melt contribute to the flow in these streams. During 15–18 June 2013 a highly critical meteorological condition was initiated to develop a very low-pressure area over the Himalaya region of Uttarakhand in India due to the convergence of a SW monsoon trough and westerlies that led to the development of dense rainy clouds in the area (Mehta et al. 2016). According to the Indian Meteorological Department (IMD) the rainfall in the region between 15–18 June 2013 was 385.1 mm against the normal of 71.3 mm; enlargement of about 440%. In the same period UAB has also faced heavy flood, affected more than 4.4 km^2 area along the Laxman Ganga (originates from Tipra Glacier) (SB5), Khiro Ganga (originates from Panpatiya Glacier) (SB4) and Alaknanda river between Benakuli and Govind Ghat of the study area. Five major villages in the UAB, namely Bhyundhar (2500 m asl), Benakuli (2400 m asl), Lambaghar (2300 m asl), Govind Ghat (1700 m asl) and Pulna (2000 m asl) along with a major Hydroelectric project at Lambaghar was razed out and completely filled with huge amount of sediment and debris (Mehta et al. 2016).

2.2 Percent of glacierized and snow cover area in the basin

Randolph glacier inventory (Pfeffer et al. 2014) have been used to calculate the glacierized area percentage in the basin for the year 2014. Total glacierized area in UAB is ∼ 358.2 km^2, i.e. 23.4% of the total area in the UAB. There are 16 major glaciers in the UAB, namely Satopanth, Bhagirath Kharak, Bhagnyu, Arwa, Tara Bamak, Ragas, Baibala Bamak, Uttri Chamrao, Dakhini Chamrao, Pachim Kamet, Uttari Kamet, Dakhini Nagthuni, Anadardip, Khuliya Garvya, Panpatiya and Tipra (Fig. 1). There are 20 numbers (> 1 km^2) of glaciers on the right bank of Saraswathi and Alaknanda river which comprises of about 61% (218.7 km^2) of total glacierized area in UAB, whereas there are 16 (> 1 km^2) number of glaciers on the left bank of Saraswathi and Alaknanda river comprises about 39% (139.5 km^2) of glacierized area.

2.3 Geology

The study area is distinguished by Higher Himalayan crystalline rocks of the Vaikrita group. There are four geological formations under Vaikrita group viz. Martoil Formation, Pindari Formation, Pandukeshwar Formation and Joshimath Formation. The Higher Himalayan crystalline consists of high-grade metamorphic rocks like granites, gneisses, quartzite, metabasics and high-grade schists (Valdiya 1987, 1999a; Ahmad et al. 2000) (Table 1 and Fig. 2f).

3 Methodology

The drainage network has been delineated by using the Cartosat-1 Digital Elevation Model (DEM) obtained from Bhuvan, ISRO, with a surface pixel resolution of 32 m (Fig. 2a). The DEM was analysed to extract the morphometric and morphotectonic parameters, and finally divide it into 10 sub-basins (Fig. 2b). In the study, only those sub-basins have been

Table 1 Geological group its formation and lithology in Upper Ganga basin (after Valdiya 1999a, b)

Vaikrita group	Lithology
Martoil Formation	Tourmaline granite/porphyro- blastic, biotite schists and injection gneiss
Pindari Formation	Calc silicate, lucocratic gneiss with intercalation of garnet mica schist
Pandukeshwar Formation	White quartzite with inter bands of garnet kyanite mica schist. Kyanite/garnet mica schist with pigmatite and aplite vein and calc silicate rocks and gneiss
Joshimath Formation	Augen genisses/banded and porphyroblasts with pigmatic vein and granite instruction

considered, which consists of at least three different orders of streams. Subsequently, 50 parameters of morphometry and 6 parameters of morphotectonic have been determined for UAB and its sub-basins.

3.1 Morphometric parameters

The morphometric parameters were evaluated from two different parameters, i.e. basin parameters and calculated parameters. Various parameters within these two aspects were then analysed and associated to recognize how they interact and affect each other. The overall morphometric parameters are divided into four different classes, namely drainage network, basin geometry, drainage texture and relief characteristics, which has been analysed in accordance to traditional morphometric laws (Horton 1945; Strahler 1964).

Under the drainage network class, there are 12 different parameters (Table 2 and 3). Stream ordering is defined as the hierarchical role of stream within a drainage basin (Bali et al. 2012). The ordering of the streams starts from the topmost tributaries that do not have their own feeders (Strahler 1952a, b). Surface runoff characteristics of the basin can be clearly understood with stream length of the drainage. The entire length of individual ordered stream has been calculated by adding the length of all streams on the basin. Stream length ratio (Lurm) is defined as the ratio of the mean length of the higher order to the next lower order of stream (Horton 1945). Bifurcation ratio (Rb) is referred as the ratio of total number of stream segments of lower order to subsequent higher order (Schumm 1956). Rb has an inverse correlation with the permeability and high Rb suggests flash flooding potential during storm events leading to deterioration of the top soil. (Howard 1990). The Rho coefficient is generally defined as the ratio between stream length and bifurcation ratio and defines the association between the physiographical development and the drainage density of the basin (Horton 1945). Rho also enables the assessment of the storage capacity of the drainage network, whereas channel index and valley index are defined as the ratio of main channel length to minimum aerial distance and ratio of valley length to the minimum aerial distance, respectively.

There are 22 different parameters under the basin geometry morphometric class (Table 3). The Drainage texture (Dt) is known as the ratio between total number of stream segments of all orders to the basin perimeter (Horton 1945). Dt generally dependent on a number of factors such as climate, precipitation, vegetation, rock and soil composition, potential for infiltration, relief and development stage of the basin (Smith 1950). The values of Dt are classified as: very fine (> 8), fine (6–8), moderate (4–6), coarse (2–4) and very coarse (< 2) (Smith 1950). Elongation ratio (Re) is defined as the ratio of diameter of a circle of the basin to the maximum basin length. Re value ranges between 0 (highly

elongated shape) to 1 (round shape). Wandering ratio (Rw) is the ratio of main channel length to the valley length, whereas texture ratio (Rt) is the ratio of first-order stream to the perimeter of the basin, which depends on the underlying lithology, infiltration capacity and relief aspects of the terrain. Hydraulic sinuosity index (Hsi) and Topographic sinuosity index (Tsi) deals with the development of the flood plains and flow of natural stream courses in the basin, respectively (Pareta and Pareta 2011).

Drainage texture and relief class consist of 7 and 9 number of morphometric parameters, respectively (Table 3). Stream frequency (Fs) is described as the ratio between stream numbers segments and total area of the basin, which is also correlated with infiltration capacity, permeability and relief of the sub-basins (Horton 1932; Vijith and Satheesh 2006; Bali et al. 2012). The Drainage density (Dd) indicates the intimacy of spacing between the channels within a basin (Horton 1932). It is one of the key indicators to provides a dimension of divisions in the landscape and runoff potential (Vijith and Satheesh 2006). Drainage density is sensitive to surface and sub-surface geology, climate, vegetation and lithology of the area (Strahler 1952a, b; Melton 1957). The increase in drainage density indicates high flood and reduction in drainage density usually shows declining flood volumes (Pallard et al. 2009). Drainage intensity (Di) defines the ratio of stream frequency to drainage density, low value of Di indicates less surface runoff making it highly susceptible to flooding, gully erosion and landslide (Faniran 1968). Relief ratio (Rhl) is the ratio of the total basin relief to the length of the basin. Low value of Rhl indicates lower slope and high resistive basement rocks in the basin.

3.2 Morphotectonic parameters

Six major morphotectonic parameters (Basin elongation ratio, Hypsometric curve and Hypsometric integral, Basin asymmetry factor, Mountain front sinuosity, Basin shape and Valley floor width to height ratio) were analysed for the UAB and its sub-basins by calculating various geomorphic indices (Table 4, Figs. 3 and 4). The basin elongation ration (Re) indicates recent tectonic activity in the basin and it defines as the ratio of basin area to its length (Table 4) (Cannon 1976; Bull and McFadden (1977). Basin having arid to semi-arid climatic conditions displays Re values < 0.50, between 0.50 and 0.75 and > 0.75 for tectonically active, slightly active and inactive settings, respectively.

Basin asymmetry factor (Af) is a method defined for detecting transverse tectonic tilting to the flow in the basin (Hare and Gardner 1985; Keller and Pinter 2002). The Af is susceptible to change in a direction perpendicular to the direction of the flow in channel and is defined as the ratio between basin area in the right bank of the main channel to the total area of the basin (Table 4) (Hamdouni et al. 2008; Sajadi et al. 2019). Af values close to 50 specifies the symmetric condition in the basin, indicating no tilting. Af > 50 indicates that the basin tilted leftward from its main trunk and Af < 50 shows that basin tilted towards right with respect to its main trunk (Hare and Gardner 1985; Keller and Pinter 2002; Sajadi et al. 2019). For the purpose of evaluating the relative active tectonics, the values of Af is affiliated as 'Af-50', which indicates the difference between the neutral value (50) and the observed value.

Mountain front sinuosity (Smf) defines the relative tectonic activity across the mountain front (Table 4) (Bull 1977; Keller and Pinter 2002; El Hamdouni et al. 2008; Pérez-Peña et al. 2010). Smf refers to the degree of slope and stream interactions that produce irregular (sinuous) front and vertical tectonic activity resulting in the development of prominent straight front (Ramírez-Herrera 1998; Sajadi et al. 2019). Bull (1977)

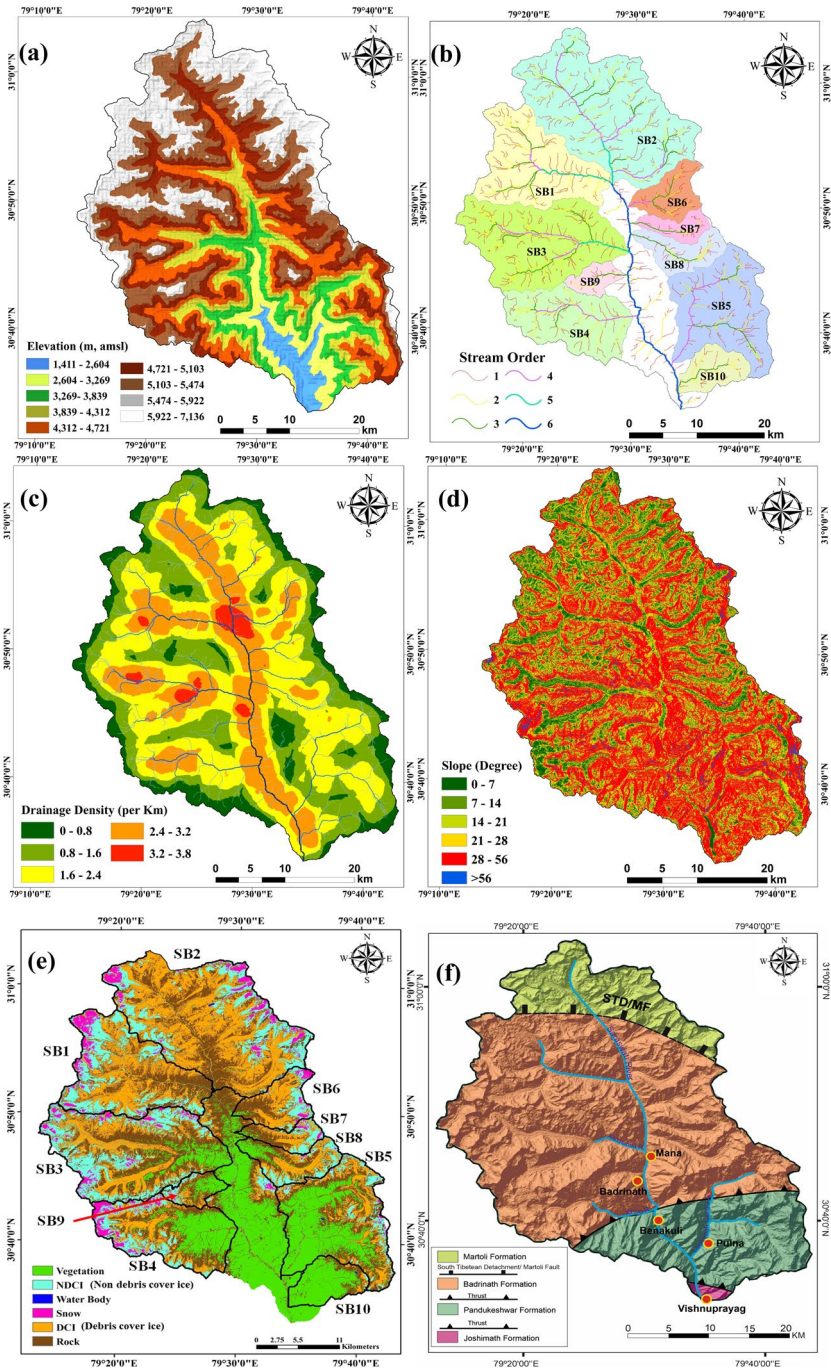Fig. 2 **a** Digital elevation map, **b** Sub-basins and stream order, **c** drainage density map, **d** slope map, **e** supervised Landcover map of Upper Alaknanda river basin and **f** geological map of UAB basin (after Valdiya 1999a, b; Ahmad et al. 2000)

categorised the values of Smf into three different groups; Smf < 1.4 indicates tectonically active front, Smf < 3 and > 1.4 indicates less active while Smf > 3 is considered as inactive mountain fronts.

Hypsometric curves (HC) and hypsometric integrals are defined as the two important parameters of watershed environments (Ritter et al. 2002). Hypsometric analysis helps to develop a connection in-between horizontal cross-sectional area and elevation (Singh et al. 2008). HC plays an important tool to understand the past soil movement of the basins under similar hydro-geological conditions in different drainage basins. According to Strahler (1952a, b) the shapes of the HC are classified as; youth (convex upward curves, defining stabilized basin), mature (S-shaped hypsometric curves that is convex downwards at low elevations and concave upwards at high elevations) and peneplain or distorted (concave upward curves, indicating more vulnerability of basin to the erosion processes) (Fig. 3). The hypsometric integral (HI) is defined as the geomorphological parameter, classified under different geologic stages during basin development. The area below the HC is defined as the hypsometric integral (HI) and is measured by:

$$\text{Hypsometric Integral} = \frac{(\text{Mean elevation} - \text{Minimum elevation})}{(\text{Maximum elevation} - \text{Minimum elevation})}$$

The HI is expressed in percentage, and defines the difference of the present volume associated to the original volume of the basin (Ritter et al. 2002) or it estimates the volume that has not been eroded (El Hamdouni et al. 2008). According to Bishop (2002), the HI explains the hydrological processes and land degradation factor that has experienced during the different geological time. HI also helps to explain the amount of surface runoff and sediment yield from the basin (Sarangi and Bhattacharya 2000; Jain et al. 2001; Singh et al. 2008). Hypsometric curve for UAB has been computed along with hypsometric integral (HI) values for all the 10 sub-basins.

Basin shape index (Bs) is defined as the ratio of basin length to basin width (Cannon 1976). The valley floor width to height ratio (Vf) is used to differentiate mountain features carved by glaciers (broad, U-shaped valleys) and those carved by streams (tight, V-shaped valleys). However, this index has also been used to identify parts of the mountain front that is experiencing or undergoing tectonic activities. Large values of Vf suggest broader U-shaped valleys and are suggestive of areas having dormant tectonic activities due to the availability of lateral erosion (Mayer 1986). The Vf also defines whether the stream is cutting downward or eroding across into adjacent hill slopes. Vf values < 0.25 is defined as highly active, Vf values between 0.25 and 0.40 suggest moderately active regions and Vf values greater than 0.40 is classified as low active. Finally, the cumulative analysis of morphotectonic parameters is carried out to obtained the Relative Tectonic Activity Index (Iat). Three different ranks have been assigned according to decreasing uplift rates for all the six morphotectonic parameters referred in Table 5 (Bull and McFadden 1977). Relative Tectonic Activity Index (Iat) is categorized in four classes as per El Hamdouni et al. (2008) and Anand and Pradhan (2019). The Iat distribution has been classified as: (1) very high tectonically active ($S/n < 1.97$), (2) high tectonically active ($S/n = 1.97–2.05$), (3) Moderate tectonically active ($S/n = 2.05–2.21$) and (4) Low tectonically active ($S/n > 2.21$). The high Iat value of the basin indicates low tectonic activity and low Iat value indicates the highly tectonic active region (Table 5).

The cloud-free Landsat and Google earth image has been also analysed to mark the triangular facets in the study area, which represent the relative tectonic activity (Fig. 7).

Table 2 Basin parameters of the Upper Alaknanda river basin and its sub-basins

S. No.	Stream Number		SB1	SB2	SB3	SB4	SB5	SB6	SB7	SB8	SB9	SB10	UAB
Area			190.5	352.3	239.5	145.6	192.7	55.4	31.4	56.2	27.3	51.4	1527
Perimeter			77.3	99.7	81.1	61.1	77.0	38.3	33.4	42.6	28	33.6	199
Stream order (Nu)		$N1$	97	178	128	68	98	34	22	35	16	23	784
		$N2$	24	44	32	18	22	7	4	8	4	6	189
		$N3$	6	13	8	3	4	2	1	1	1	1	39
		$N4$	2	4	2	1	1	1					11
		$N5$	1	1	1								3
		$N6$											1
$\sum$ Nu			130	240	171	90	125	44	27	44	21	30	1027
Stream length		$N1$	126.6	196.5	152.8	75.2	94.1	28.4	13.1	26.9	14	18.7	827
		$N2$	38.9	95.4	54.7	45.0	41.7	13.9	10.3	18.1	5	14.0	369
		$N3$	24.7	41.2	26.7	7.0	24.3	9.1	8.9	12.8	11	10.9	166
		$N4$	5.1	37.9	20.3	18.2	18.5	4.5					104
		$N5$	12.7	7.5	8.61								29
		$N6$											41
$\sum$ Lu			208.1	378.4	263.0	145.4	178.6	55.9	32.3	57.9	30.2	43.6	1536
Stream length ratio (Lurm)		$N1$											
		$N2$	6.5	4.1	5.6	3.3	4.5	4.1	2.5	3.0	5.0	2.7	4.5
		$N3$	2.4	3.5	3.1	9.6	2.6	2.3	1.8	2.1	0.7	1.9	3.3
		$N4$	6.4	1.4	1.8	0.5	1.7	2.7					2.1
		$N5$	0.5	6.3	2.9								4.5
		$N6$											0.8
	Total		15.8	15.4	13.4	13.5	8.8	9.1	4.3	5.1	5.8	4.6	15.3
	Mean		3.9	3.8	3.3	4.5	2.9	3.0	2.1	2.5	2.9	2.3	3.1

Table 2 (continued)

S. No.	Stream Number	SB1	SB2	SB3	SB4	SB5	SB6	SB7	SB8	SB9	SB10	UAB
Bifurcation ratio (Rb)												
	N1											
	N2	4.0	4.0	4.0	3.8	4.5	4.9	5.5	4.4	4	3.8	4.1
	N3	4.0	3.4	4.0	6.0	5.5	3.5	4	8.0	4	6.0	4.8
	N4	3.0	3.3	4.0	3.0	4.0	2.0					3.5
	N5	2.0	4.0	2.0								3.7
	N6											3.0
	Total	13.0	14.7	14.0	12.8	14.0	10.4	9.5	12.4	8.0	9.8	19.2
	Mean	3.3	3.7	3.5	4.3	4.7	3.5	4.8	6.2	4.0	4.9	3.8

Table 3 Morphometric parameters on the basis of drainage network, basin geometry, drainage texture and relief characteristics

Drainage network

Parameter			SB1	SB2	SB3	SB4	SB5	SB6	SB7	SB8	SB9	SB10	UAB
Stream number (Nu)	$Nu = N1 + N2\ldots + Nn$	Strahler (1964)	130	240	171	90	125	44	27	44	21	30	1027
Stream length (Lu)	$Lu = L1 + L2\ldots + Ln$		208.1	378.4	263.0	145.4	178.6	55.9	32.3	56	30	44	1536.0
Mean stream length ratio (Lurm)		Horton (1945)	3.9	3.8	3.3	4.5	2.9	3	2.5	2.5	2.9	2.3	3.1
Weighted mean stream length ratio (Luwm)		Horton (1945)	5.6	4.8	3.7	7.9	3.2	3.1	2.5	2.6	4.3	2.3	3.1
Mean bifurcation ratio (Rbm)			3.2	3.6	3.5	4.2	4.6	3.5	4.8	6.2	4	4.9	3.8
Weighted mean bifurcation ratio (Rbwm)			3.9	3.9	4.0	4.1	4.6	4.5	5.3	5	4	4.3	4.2
Main channel length (Cl)	ArcGis	Horton (1945)	27.4	30.5	30	26	25.4	15	15.1	13	15.5	13.9	71.5
Rho coefficient (ρ)	$\rho = Lur/Rb$		1.2	1.0	1.0	1.1	0.6	0.9	0.5	0.4	0.7	0.5	0.8
Valley length (Vl)	ArcGis		18.8	23.8	22.5	18.9	20	13	11.8	14	9.5	11	58.6
Minimum aerial distance (Adm)	ArcGis		17.5	22.2	20.1	17.5	17	11	10.6	12	8.3	8.8	57.6
Channel index (Ci)	$Ci = Cl/Adm$		1.6	1.4	1.5	1.5	1.5	1.4	1.4	1.1	1.9	1.6	1.2
Valley index (Vi)	$Vi = Vl/Adm$		1.1	1.1	1.1	1.1	1.2	1.2	1.1	1.2	1.1	1.2	1.0

Basin geometry

Parameter		SB1	SB2	SB3	SB4	SB5	SB6	SB7	SB8	SB9	SB10	UAB
Basin length (Lb)	ArcGis	18.8	23.8	22.5	18.9	20.0	12.6	11.8	13.9	9.5	10.9	58.6
Basin width (Wb)	ArcGis	15.3	17.1	13.2	10.5	21.0	7.2	4.9	5.9	5.5	7.1	35.0
Basin area (A) Sq	ArcGis	190.5	352.3	239.5	145.6	192.7	55.4	31.4	56.2	27.3	51.4	1527.0
Basin perimeter (P)	ArcGis	77.3	99.7	81.1	61.1	77.0	38.3	33.4	42.6	28	33.6	199.0
Relative perimeter (Pr)	$Pr = A/P$	2.5	3.5	3.0	2.4	2.5	1.4	0.9	1.3	1.0	1.5	7.7
Length area relation (Lar)	$Lar = 1.4 * A^{0.6}$	32.7	47.2	37.5	27.8	32.9	15.6	11.1	15.7	10.2	14.9	113.9
Lemniscate's (k)	$k = Lb2/A$	1.9	1.6	2.1	2.5	2.1	2.9	4.4	3.4	3.3	2.3	2.2
Form factor ratio (Ff)	$Ff = A/Lb^2$	0.5	0.6	0.5	0.5	0.5	0.3	0.2	0.3	0.3	0.4	0.4
Shape factor ratio (Rs)	$Sf = Lb2/A$	1.9	1.6	2.1	2.5	2.1	2.9	4.4	3.4	3.3	2.3	2.2

3275

Table 3 (continued)

Basin geometry

Parameter			SB1	SB2	SB3	SB4	SB5	SB6	SB7	SB8	SB9	SB10	UAB
Elongation ratio (Re)	$Re = 2/Lb * (A/\pi)^{0.5}$	Schumm (1963)	3.2	4.7	3.4	2.5	3.1	1.4	0.8	1.3	0.9	1.5	8.3
Length width ratio			1.2	1.4	1.7	1.8	1.8	1.75	2.4	2.4	1.7	1.5	1.7
Circularity ratio (Rc)	$Rc = 12.57 * A/P2$	Horton (1945)	0.4	0.4	0.5	0.5	0.4	0.5	0.4	0.4	0.4	0.6	0.5
Circularity ration (Rcn)	$Rcn = A/P$		2.5	3.5	3.0	2.4	2.5	1.4	0.9	1.3	1.0	1.5	7.7
Drainage texture (Dt)	$Dt = Nu/P$	Horton (1945)	1.7	2.4	2.1	1.5	1.6	1.2	0.8	1.0	0.8	0.9	5.2
Compactness coefficient (Cc)	$Cc = 0.2841 * P/A0.5$	Gravelius (1914)	1.6	1.5	1.5	1.4	1.6	1.5	1.7	1.6	1.5	1.3	1.4
Fitness ratio (Rf)	$Rf = CI/P$		0.4	0.3	0.4	0.4	0.3	0.4	0.5	0.3	0.6	0.4	0.4
Wandering ratio (Rw)	$Rw = CI/Lb$		1.5	1.3	1.3	1.4	1.4	1.2	1.3	0.9	1.6	1.3	1.2
Texture ratio (Rt)	$Rt = N1/P$	Smith (1950)	2.7	1.8	1.6	1.1	1.3	0.9	0.7	0.8	0.6	0.7	3.9
Elipticity index (Ie)	$Ie = \pi * VI2/4A$		1.5	1.3	1.7	1.9	1.6	2.3	3.5	2.7	2.6	1.8	1.8
Hydraulic sinuosity index (Hsi) %	$His = \{(Ci - Vi)/(Ci - 1)\} * 100$		86.9	80.7	75.9	83.5	64.3	57.8	73.3	78.2	83.3	59.1	92.8
Topographic sinuosity index (Tsi) %	$Tsi = \{(Vi - 1)/(Ci - 1)\} * 100$		13.1	19.3	24.1	16.5	35.7	42.2	26.7	21.8	16.7	40.9	7.2
Standard sinuosity index (Ssi)	$Ssi = Ci/Vi$		1.5	1.3	1.3	1.4	1.3	1.2	1.3	0.9	1.6	1.9	1.2

Drainage texture

Parameter			SB1	SB2	SB3	SB4	SB5	SB6	SB7	SB8	SB9	SB10	UAB
Stream frequency (Fs)	$Fs = Nu/A$	Horton (1932)	0.7	0.7	0.7	0.6	0.6	0.8	0.9	0.8	0.8	0.6	0.7
Drainage density (Dd)	$Dd = Lu/A$	Horton (1945)	1.1	1.1	1.1	1.0	0.9	1.0	1.0	1.0	1.1	0.8	1.0
Constant of channel maintenance (C)	$C = 1/Dd$		0.9	0.9	0.9	1.0	1.1	1.0	1.0	1.0	2.0	1.2	1.0
Drainage intensity (Di)	$Di = Fs/Dd$		0.6	0.6	0.7	0.6	0.7	0.8	0.8	0.8	1.5	0.7	0.7
Infiltration number (If)	$If = Fs * Dd$	Faniran (1968)	0.7	0.7	0.8	0.6	0.6	0.8	0.9	0.8	0.4	0.5	0.7
Length of overland flow (Lg)	$Lg = A/2 * Lu$		0.5	0.5	0.5	0.5	0.5	0.5	0.5	0.5	0.5	0.6	0.5

Relief characteristics

Parameter			SB1	SB2	SB3	SB4	SB5	SB6	SB7	SB8	SB9	SB10	UAB
Height of basin mouth (z)	ArcGis		3958	3958	3165	2388	1779	3694	3526	3421	3081	1666	1411

Table 3 (continued)

Drainage texture

Parameter			SB1	SB2	SB3	SB4	SB5	SB6	SB7	SB8	SB9	SB10	UAB
Maximum height of the basin (Z)	ArcGis		6309	7110	6997	6520	6710	6565	5941	5740	5468	5032	7136
Total basin relief (H)	$H = Z - z$	Schumm (1956)	2351	3152	3832	4132	4931	2871	2415	2319	2387	3366	5725
Relief ratio (Rhl)	$Rhl = H/Lb$	Schumm (1956)	125.1	132.4	170.3	218.6	246.6	227.9	204.7	166.8	251.3	308.8	97.7
Relative relief ratio (Rhp)	$Rhp = Rhl*100/P$		161.7	132.9	209.9	358.0	320.2	595.5	612.8	391.9	897.4	919.0	49.1
Gradient ratio (Rg)	$Rg = (Z - z)/Lb$		125.1	132.4	170.3	218.6	246.6	227.9	204.7	166.8	251.3	308.8	97.7
Ruggedness number (Rn)	$Rn = Dd * (H/1000)$	Strahler (1964)	2.6	3.4	4.2	4.1	4.6	2.9	2.5	2.4	1.2	2.9	5.8
Melton ruggedness number (MRn)	$MRn = H/A0.5$		170.3	167.9	247.6	342.4	355.3	385.8	431.2	309.3	457.2	469.3	146.5
Basin slope (Sw)	$Sw = H/Lb$		125.1	132.4	170.3	218.6	246.6	227.9	204.7	166.8	251.3	308.8	97.7

Table 4 Parameter estimated to compute tectonic activity in the UAB and its Sub-Basins

| S. no.	Morphotectonic parameters	Formula	References	Classes	Range of the present values
1	Basin elongation ratio (Re)	$Re = (2\sqrt{A}\sqrt{\prod}) L$, where, A = Basin area, L = Basin length	Bull and McFadden (1977)	Re < 0.50, tectonically active Re = 0.50–0.75, slightly active Re > 0.75, inactive setting	0.54–0.89
2	Asymmetry factor (Af)	AF = 100(Ar/At), Where Ar = Basin area in the right bank of main channel and At = Total area of drainage basin	Cox (1994)	AF < 50, suggest basin tilted toward right AF = 50, stable setting environment AF > 50, suggest basin tilted toward left	28.92–63.40
3	Mountain front sinuosity (Smf)	Smf = Lmf/Ls, Where Lmf = Mountain front length along mountain foot, Ls = Straight line length of mountain front	Bull and McFadden (1977)	Smf < 1.4, tectonically active Smf = 1.4–3, slightly active Smf > 3, inactive seting	1.02–1.30
4	Hypsometric integral (HI)	HI = (Elevmean − Elevmin)/(Elevmax − Elevmin)	Pike and Wilson 1971; Keller and Pinter 2002	HI > 0.5, youngest Stage HI: 0.4–0.5 intermediate stage HI < 0.4 Old stage	0.44–0.53
5	Basin shape (Bs)	Bs = Bl/Bw, where Bl = Basin length, Bw = Basin width	Cannon 1976	Bs > 2.30, tectonically active Bs 2.3–1.2, moderate active Bs < 1.2, less active	1.23–2.41
6	Valley floor width to height ratio (Vf)	Vf = 2Vw/(Eld −Esc) + (Erd −Esc) Where, Vw = width of valley floor; Eld/Erd = Elevation of left- and right-hand valley divides going down stream; and ESC = The elevation of the stream channel or valley floor	Bull (1977), Bull and McFadden (1977)	Vf < 0.25, highly active Vf = 0.25–0.40, moderate active Vf > 0.40, low active	0.15–1.01
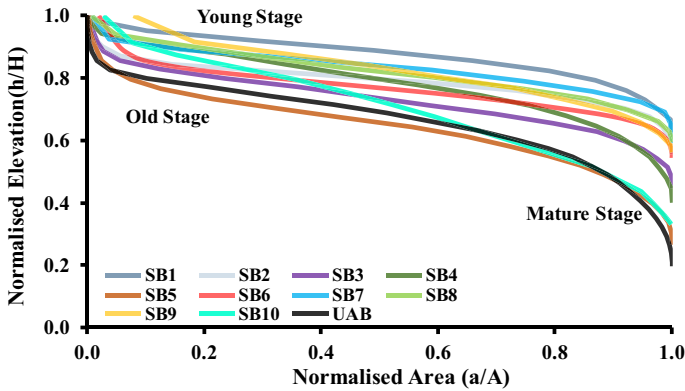
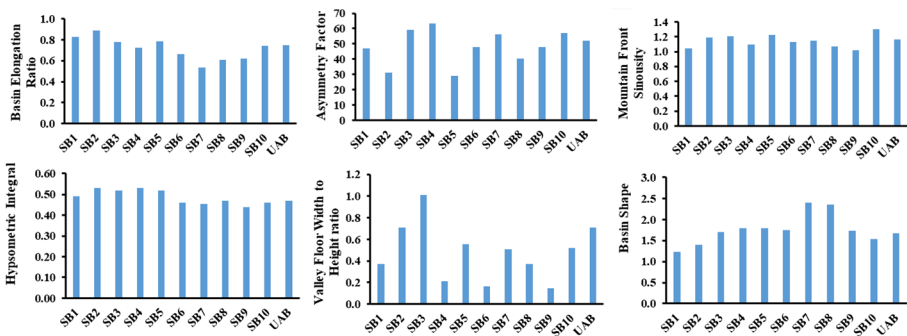**Fig. 3** Hypsometric curves for Upper Alaknanda river basin and its 10 sub-basins

Fig. 4 Bar graph representing the various morphotectonic parameters in UAB and its sub-basins

3.3 Statistical analysis

Various statistical analysis like correlation analysis, Hierarchical cluster analysis (HCA) and Principle component analysis/factor analysis (PCA) were carried out using MS Excel 2016 and SPSS (V22) to classify the similarity between different morphometric parameters and between the sub-basins (Tables 6 and 7; Figs. 5 and 6). Hierarchical cluster analysis (HCA) is a statistical technique which combines the samples with similar inherent structure and among groups depicting a hierarchy (Lee and Yang 2009). Both Q-mode and R-mode HCA have been performed to find nearness or similarity between the data sets (Fig. 6) (Vega et al. 1998). The R-mode HCA helps to classify the parameters, whereas the Q-mode HCA helps to highlight the relationship between sub-basins. PCA is a statistical tool having aim to represent variation in data set using axes as a factor (principle components, PC). PCA analysis is a multivariate statistical technique where the data set is reduced to small factors without mislaying the information. PCA analysis describes that, PC1 explains variation in most of the data in comparison to PC2, similarly PC2 explains more variation in data compare to PC3 (Granato et al. 2018). An interconnection between various parameters was identified and a correlation matrix was computed. For PCA factoring, the factors with eigenvalue > 1 were accepted to define the principal factors (Kaiser 1960). Varimax

Table 5 Calculation of relative tectonic activity index (Iat) using morphotectonic indices in UAB and its sub-basins

Morphotectonic parameters	Basin elongation ratio (Re)	Hypsometric integral (HI)	Asymmetry factor (AF-50)	Mountain front sinuosity (Smf)	Basin shape (Bs)	Valley floor width to height ratio (Vf)	S/n	Iat
SB1	0.83	0.49	− 2.79	1.04	1.23	0.37		
Rank	3	1	2	1	2	2	1.83	1
SB2	0.89	0.53	− 18.80	1.19	1.39	0.71		
Rank	3	1	1	2	2	3	2.00	2
SB3	0.78	0.52	9.28	1.21	1.70	1.01		
Rank	3	1	3	2	2	3	2.33	4
SB4	0.72	0.53	13.40	1.10	1.80	0.21		
Rank	2	1	3	1	2	1	1.67	1
SB5	0.78	0.52	− 21.08	1.22	1.80	0.55		
Rank	3	1	1	2	2	3	2.00	2
SB6	0.66	0.46	− 2.26	1.13	1.75	0.17		
Rank	2	1	2	1	2	1	1.50	1
SB7	0.54	0.45	6.07	1.15	2.41	0.51		
Rank	2	1	3	1	1	3	1.83	1
SB8	0.61	0.47	− 9.84	1.07	2.36	0.37		
Rank	2	1	1	1	1	2	1.33	1
SB9	0.62	0.44	− 1.96	1.02	1.73	0.15		
Rank	2	2	2	1	2	1	1.67	1
SB10	0.74	0.46	7.10	1.30	1.54	0.52		
Rank	3	1	3	1	2	3	2.17	3
UAB	0.75	0.47	2.17	1.16	1.67	0.71		
Rank	3	1	2	1	2	3	2.00	2

Where S = Re + HI + AF + Smf + Bs + Vf and n = number of parameters

Table 6 Correlation matrix of the morphometric parameters in the Upper Alaknanda river basin

	Nu	Lu	Lurm	Luwm	Rbm	Rbwm	Cl	ρ	Vl	Adm	Ci	Vi	Lb	Wb	A Sq	P	Pr	Lar	k	Ff	Rs	Re	Rc	Rcn
Nu	1.0																							
Lu	1.0	1.0																						
Lurm	0.6	0.6	1.0																					
Luwm	0.4	0.4	0.9	1.0																				
Rbm	−0.5	−0.5	−0.6	−0.4	1.0																			
Rbwm	−0.6	−0.6	−0.7	−0.6	0.7	1.0																		
Cl	0.9	0.9	0.8	0.6	−0.6	−0.6	1.0																	
ρ	0.6	0.7	0.9	0.8	−0.9	−0.8	0.8	1.0																
Vl	1.0	0.9	0.7	0.4	−0.4	−0.5	0.9	0.6	1.0															
Adm	1.0	1.0	0.7	0.5	−0.5	−0.5	1.0	0.7	1.0	1.0														
Ci	−0.2	−0.1	0.1	0.2	−0.5	−0.5	0.1	0.2	−0.3	−0.2	1.0													
Vi	−0.6	−0.6	−0.8	−0.7	0.6	0.4	−0.7	−0.8	−0.6	−0.7	−0.1	1.0												
Lb	1.0	0.9	0.7	0.4	−0.4	−0.5	0.9	0.6	1.0	1.0	−0.3	−0.6	1.0											
Wb	0.8	0.8	0.5	0.3	−0.4	−0.4	0.8	0.5	0.8	0.8	0.0	−0.4	0.8	1.0										
A Sq	1.0	1.0	0.6	0.4	−0.5	−0.6	0.9	0.6	1.0	1.0	−0.1	−0.6	1.0	0.8	1.0									
P	1.0	1.0	0.6	0.4	−0.5	−0.5	0.9	0.7	1.0	1.0	−0.2	−0.6	1.0	0.9	1.0	1.0								
Pr	1.0	1.0	0.7	0.4	−0.5	−0.6	0.9	0.7	1.0	1.0	−0.1	−0.5	1.0	0.8	1.0	1.0	1.0							
Lar	1.0	1.0	0.7	0.4	−0.5	−0.6	0.9	0.7	1.0	1.0	−0.1	−0.6	1.0	0.9	1.0	1.0	1.0	1.0						
k	−0.8	−0.8	−0.6	−0.4	0.5	0.8	−0.8	−0.6	−0.7	−0.7	−0.1	0.2	−0.7	−0.8	−0.8	−0.8	−0.9	−0.8	1.0					
Ff	0.9	0.9	0.7	0.5	−0.5	−0.7	0.9	0.7	0.8	0.8	0.1	−0.4	0.8	0.8	0.9	0.9	0.9	0.9	−1.0	1.0				
Rs	−0.8	−0.8	−0.6	−0.4	0.5	0.8	−0.8	−0.6	−0.7	−0.7	−0.1	0.2	−0.7	−0.8	−0.8	−0.8	−0.9	−0.8	1.0	−1.0	1.0			
Re	0.9	0.9	0.6	0.4	−0.5	−0.7	0.8	0.6	0.8	0.8	0.1	−0.4	0.8	0.8	0.9	0.9	0.9	0.9	−1.0	1.0	−1.0	1.0		
Rc	−0.1	0.0	0.1	0.1	−0.1	−0.5	0.0	0.1	−0.1	−0.1	0.3	0.3	−0.1	−0.1	0.0	−0.1	0.1	0.0	−0.4	0.3	−0.4	0.3	1.0	
Rcn	1.0	1.0	0.7	0.4	−0.5	−0.6	0.9	0.7	1.0	1.0	−0.1	−0.5	1.0	0.8	1.0	1.0	1.0	1.0	−0.9	0.9	−0.9	0.9	0.1	1.0
Dt	1.0	1.0	0.6	0.4	−0.5	−0.6	0.9	0.7	1.0	1.0	−0.2	−0.6	1.0	0.8	1.0	1.0	1.0	1.0	−0.8	0.9	−0.8	0.8	0.0	1.0
Cc	0.0	0.0	−0.1	−0.2	0.2	0.5	0.0	−0.1	0.0	0.0	−0.3	−0.3	0.0	0.0	0.0	0.0	−0.2	−0.1	0.5	−0.4	0.5	−0.4	−0.5	−0.2
Rf	−0.6	−0.6	−0.1	0.1	−0.2	−0.1	−0.4	−0.1	−0.6	−0.6	0.8	0.0	−0.6	−0.6	−0.6	−0.7	−0.6	−0.6	0.5	−0.5	0.5	−0.5	0.2	−0.6
Rw	0.1	0.1	0.3	0.4	−0.6	−0.6	0.3	0.4	0.0	0.1	0.9	−0.4	0.0	0.2	0.1	0.1	0.1	0.1	−0.2	0.2	−0.2	0.2	0.1	0.1
Rt	0.7	0.8	0.6	0.4	−0.6	−0.5	0.8	0.8	0.7	0.8	0.0	−0.6	0.7	0.7	0.7	0.8	0.7	0.8	−0.7	0.8	−0.7	0.8	−0.2	0.7

Table 6 (continued)

	Nu	Lu	Lurm	Luwm	Rbm	Rbwm	Cl	ρ	Vl	Adm	Ci	Vi	Lb	Wb	A Sq	P	Pr	Lar	k	Ff	Rs	Re	Rc	Rcn
Ie	**-0.8**	**-0.8**	-0.6	-0.4	0.5	**0.8**	**-0.8**	-0.6	**-0.7**	**-0.7**	-0.1	0.2	**-0.7**	**-0.8**	**-0.8**	**-0.8**	**-0.9**	**-0.8**	**1.0**	**-1.0**	**1.0**	**-1.0**	-0.4	**-0.9**
Hsi	0.4	0.4	0.5	0.5	-0.5	-0.5	0.6	0.4	0.4	0.4	**0.6**	**-0.7**	0.4	0.4	0.4	0.4	0.4	0.4	-0.3	0.4	-0.3	0.4	0.0	0.4
Tsi	0.1	0.1	-0.2	-0.2	0.1	0.0	0.2	-0.3	0.1	0.0	0.4	0.2	0.1	0.3	0.1	0.1	0.2	0.1	-0.2	0.2	-0.2	0.2	0.3	0.2
Ssi	-0.2	-0.2	-0.1	0.1	-0.3	-0.4	-0.1	0.0	-0.3	-0.3	**0.8**	0.1	-0.3	-0.1	-0.1	-0.2	-0.1	-0.2	-0.2	0.2	-0.2	0.2	**0.7**	-0.1
Fs	-0.4	-0.4	-0.4	-0.4	0.1	0.6	-0.5	-0.3	-0.4	-0.4	-0.2	0.0	-0.4	-0.5	-0.4	-0.4	-0.5	-0.5	**0.8**	**-0.7**	**0.8**	**-0.7**	**-0.7**	-0.5
Dd	0.5	0.5	0.3	0.1	-0.1	0.1	0.5	0.3	**0.6**	**0.6**	**-0.7**	-0.3	**0.6**	0.4	0.5	0.6	0.5	0.5	-0.3	0.4	-0.3	0.3	-0.2	0.5
C	-0.4	-0.4	-0.3	0.0	0.0	-0.2	-0.4	-0.2	-0.6	-0.5	**0.7**	0.2	-0.6	-0.4	-0.4	-0.5	-0.5	-0.5	0.3	-0.4	0.3	-0.3	0.1	-0.5
Di	-0.5	-0.5	-0.3	-0.1	0.0	0.0	-0.5	-0.3	**-0.6**	-0.6	0.6	0.1	**-0.6**	-0.5	-0.5	-0.6	-0.6	-0.6	0.5	-0.5	0.5	-0.5	-0.1	-0.6
If	0.2	0.2	0.0	-0.2	0.0	0.4	0.1	0.1	0.3	0.3	0.6	-0.3	0.3	0.0	0.2	0.2	0.1	0.2	0.2	-0.1	0.2	-0.1	-0.5	0.1
Lg	0.3	0.2	-0.3	-0.5	0.0	-0.3	0.1	-0.1	0.1	0.1	**-0.7**	0.4	0.1	0.4	0.3	0.2	0.3	0.3	-0.5	0.4	-0.5	0.5	0.3	0.3
z	0.3	0.3	0.2	0.1	-0.4	-0.1	0.1	0.4	0.1	0.2	-0.3	-0.5	0.1	-0.1	0.2	0.2	0.1	0.1	0.1	0.0	0.1	0.0	-0.5	0.1
Z	**0.8**	**0.8**	**0.6**	0.4	-0.5	-0.3	**0.8**	**0.7**	**0.9**	**0.9**	-0.3	**-0.6**	**0.9**	**0.7**	**0.8**	**0.8**	**0.8**	**0.8**	-0.5	0.6	-0.5	0.6	-0.2	**0.8**
H	0.4	0.4	0.3	0.2	-0.1	-0.2	0.5	0.1	0.5	0.5	0.0	0.0	0.5	**0.6**	0.4	0.5	0.5	0.5	-0.5	0.5	-0.5	0.4	0.3	0.5
Rhl	**-0.6**	**-0.6**	-0.5	-0.3	0.3	0.2	-0.5	-0.6	**-0.6**	**-0.7**	0.4	**0.7**	**-0.6**	-0.3	**-0.6**	**-0.6**	-0.5	-0.6	0.2	**-0.6**	0.2	**-0.6**	0.6	-0.5
Rhp	**-0.8**	**-0.8**	**-0.6**	-0.4	0.3	0.3	**-0.8**	**-0.6**	**-0.9**	**-0.9**	0.5	**0.6**	**-0.9**	**-0.7**	**-0.8**	**-0.9**	**-0.8**	**-0.9**	0.5	**-0.6**	0.5	**-0.6**	0.4	**-0.8**
Rg	**-0.6**	**-0.6**	-0.5	-0.3	0.3	0.2	-0.5	-0.6	**-0.6**	**-0.7**	0.4	**0.7**	**-0.6**	-0.3	**-0.6**	**-0.6**	-0.5	-0.6	0.2	-0.4	0.2	-0.3	0.6	-0.5
Rn	0.6	0.6	0.4	0.2	-0.1	-0.1	**0.7**	0.3	**0.7**	**0.7**	-0.3	-0.2	**0.7**	**0.7**	**0.6**	**0.7**	**0.7**	**0.7**	-0.5	0.6	-0.5	0.5	0.2	**0.7**
MRn	**-0.9**	**-0.9**	**-0.6**	-0.4	0.4	0.5	**-0.8**	**-0.7**	**-0.8**	**-0.9**	0.3	**0.6**	**-0.8**	**-0.6**	**-0.8**	**-0.9**	**-0.8**	**-0.8**	**0.6**	**-0.7**	**0.6**	**-0.7**	0.3	**-0.8**
Sw	**-0.6**	**-0.6**	-0.5	-0.3	0.3	0.2	-0.5	-0.6	**-0.6**	**-0.7**	0.4	**0.7**	**-0.6**	-0.3	**-0.6**	**-0.6**	-0.5	-0.6	0.2	-0.4	0.2	-0.3	0.6	-0.5

Table 6 (continued)

	Dt	Cc	Rf	Rw	Rt	Ie	Hsi	Tsi	Ssi	Fs	Dd	C	Di	If	Lg	z	Z	H	Rhl	Rhp	Rg	Rn	MR	Sw
Dt	**1.0**																							
Cc	−0.1	**1.0**																						
Rf	**−0.6**	−0.1	**1.0**																					
Rw	0.1	−0.1	**0.6**	**1.0**																				
Rt	**0.7**	0.1	−0.5	0.2	**1.0**																			
Ie	**−0.8**	0.5	0.5	−0.2	**−0.7**	**1.0**																		
Hsi	0.3	0.0	0.3	**0.8**	0.4	−0.3	**1.0**																	
Tsi	0.0	−0.2	0.1	0.3	−0.1	−0.2	0.5	**1.0**																
Ssi	−0.2	**−0.6**	**0.6**	**0.6**	−0.1	−0.2	0.5	**0.6**	**1.0**															
Fs	−0.4	**0.7**	0.2	−0.2	−0.3	**0.8**	−0.4	−0.5	−0.5	**1.0**														
Dd	**0.6**	0.2	**−0.7**	−0.5	0.5	−0.3	−0.1	−0.2	−0.5	0.0	**1.0**													
C	−0.5	−0.1	**0.8**	**0.6**	−0.5	0.3	0.2	0.1	0.5	0.0	**−1.0**	**1.0**												
Di	**−0.6**	0.1	**0.8**	0.5	−0.5	0.5	0.1	−0.1	0.2	0.1	**−0.9**	**0.9**	**1.0**											
If	0.3	0.5	−0.5	**−0.6**	0.3	0.2	−0.3	−0.4	**−0.7**	0.4	**0.8**	**−0.8**	−0.5	**1.0**										
Lg	0.2	−0.3	−0.3	0.1	0.3	−0.5	0.1	**0.6**	0.5	0.5	−0.1	0.0	−0.2	−0.3	**1.0**									
z	0.2	0.5	−0.2	−0.1	0.4	0.1	−0.1	**−0.7**	−0.5	**0.6**	0.4	−0.2	0.0	**0.6**	−0.3	**1.0**								
Z	**0.9**	0.1	−0.5	0.0	**0.6**	−0.5	0.2	−0.2	−0.5	0.0	**0.6**	−0.5	−0.5	0.5	−0.2	0.3	**1.0**							
H	0.4	−0.4	−0.2	0.1	0.1	−0.5	0.2	0.5	0.2	**−0.6**	0.1	−0.2	−0.4	−0.2	0.2	**−0.7**	0.4	**1.0**						
Rhl	**−0.6**	−0.5	0.5	0.2	**−0.7**	0.2	−0.1	0.5	**0.6**	−0.2	**−0.6**	0.5	0.3	**−0.6**	0.2	**−0.8**	**−0.6**	0.3	**1.0**					
Rhp	**−0.9**	−0.3	**0.7**	0.2	**−0.8**	0.5	−0.2	0.2	**0.6**	0.1	**−0.8**	**0.7**	**0.6**	−0.5	0.1	−0.4	**−0.8**	−0.3	**0.8**	**1.0**				
Rg	**−0.6**	−0.5	0.5	0.2	**−0.7**	0.2	−0.1	0.5	**0.6**	−0.2	**−0.6**	0.5	0.3	**−0.6**	0.2	**−0.8**	**−0.6**	0.3	**1.0**	**0.8**	**1.0**			
Rn	**0.6**	−0.2	−0.5	−0.1	0.3	−0.5	0.1	0.3	−0.2	−0.5	0.5	**−0.6**	**−0.7**	0.2	0.1	−0.4	**0.7**	**0.9**	−0.1	**−0.6**	−0.1	**1.0**		
MRn	**−0.9**	−0.2	**0.7**	0.1	**−0.9**	**0.6**	−0.2	0.3	0.4	0.2	**−0.7**	**0.6**	0.5	−0.4	−0.1	−0.5	**−0.7**	0.0	**0.9**	**0.9**	**0.9**	−0.3	**1.0**	
Sw	**−0.6**	−0.5	0.5	0.2	**−0.7**	0.2	−0.1	0.5	**0.6**	−0.2	**−0.6**	0.5	0.3	**−0.6**	0.2	**−0.8**	**−0.6**	0.3	**1.0**	**0.8**	**1.0**	−0.1	**0.9**	**1.0**

Bold numbers represents the strong positive or negative correlation between the parameters

Table 7 Principle component analysis of the various morphometric parameters in Upper Alaknanda river basin

Parameters	PC1	PC2	PC3	PC4	PC5	PC6	PC7
Stream number	**.837**	− .239	.446	.185	− .049	− .065	.031
Stream length	**.846**	− .228	.432	.189	− .046	− .063	.034
Mean stream length ratio	.488	.293	**− .620**	.295	.408	− .057	− .168
Weighted mean stream length ratio	.236	.371	− .521	.407	.495	− .087	− .264
Mean bifurcation ratio	− .493	− .408	.304	− .426	.011	− .042	− .327
Weighted mean bifurcation ratio	− .513	**− .705**	.216	− .303	.075	.169	− .058
Main channel length	**.911**	− .138	.323	.209	.037	.025	.007
Rho coefficient	.548	.341	**− .626**	.362	.153	− .079	.100
Valley length	**.892**	− .235	.360	.133	.019	− .027	− .014
Minimum aerial distance	**.887**	− .235	.357	.168	.023	− .030	.001
Channel index	− .350	**.763**	.040	.441	− .054	.258	.065
Valley index	**− .728**	.138	.170	− .548	− .191	− .207	− .086
Basin length	**.892**	− .235	.360	.133	.019	− .027	− .014
Basin width	**.920**	− .056	.269	.022	− .099	.112	− .169
Basin area	**.838**	− .229	.450	.183	− .041	− .066	.022
Basin perimeter	**.947**	− .169	.247	.098	− .049	.025	− .033
Relative perimeter	**.934**	− .127	.315	.097	− .002	− .037	.000
Length area relation	**.922**	− .168	.324	.121	− .030	− .020	− .007
Lemniscate's	**− .717**	− .576	.227	.253	.117	.106	.089
Form factor ratio	**.718**	.521	− .375	− .219	− .048	.038	− .073
Shape factor ratio	**− .717**	− .576	.227	.253	.117	.106	.089
Elongation ratio	**.758**	.502	− .283	− .239	− .171	.035	− .038
Length width ratio	− .520	**− .744**	.213	− .090	.248	.141	− .161
Circularity ratio	.194	**.612**	.417	− .213	.243	− .486	.217
Circularity ration	**.934**	− .127	.315	.097	− .002	− .037	.000
Drainage texture	**.924**	− .188	.299	.121	− .030	− .036	.025
Compactness coefficient	− .252	**− .621**	− .374	.169	− .233	.512	− .165
Fitness ratio	− .535	.309	.332	**.650**	.201	.105	.157
Wandering ratio	− .035	**.686**	− .034	.579	.006	.401	− .024
Texture ratio	**.920**	− .121	.078	.197	− .143	− .026	.104
Ellipticity index	**− .717**	− .576	.227	.253	.117	.106	.089
Hydraulic sinuosity index	.462	.401	.097	.430	.142	.570	.085
Topographic sinuosity index	− .160	.531	.265	− .416	.077	.647	.066
Standard sinuosity index	− .199	**.834**	.305	.077	− .009	.089	.333
Stream frequency	− .475	**− .686**	− .145	.333	− .195	.104	.175
Drainage density	.479	− .428	− .487	− .445	.231	.022	.286
Constant of channel maintenance	− .456	.393	.379	.561	− .275	.002	− .255
Drainage intensity	− .554	.120	.272	**.642**	− .315	.038	− .180
Infiltration number	.127	**− .738**	− .466	− .237	.097	.075	.354
Length of overland flow	.313	.408	.320	− .453	**− .612**	.085	.167
Height of basin mouth	− .267	− .236	**− .809**	.215	− .262	− .032	.255
Maximum height of the basin	**.791**	− .186	− .294	.008	.152	.143	− .108
Total basin relief	**.703**	.081	.488	− .173	.309	.113	− .276
Relief ratio	**− .723**	.486	.334	− .242	.177	.002	− .096

Table 7 (continued)

Parameters	PC1	PC2	PC3	PC4	PC5	PC6	PC7
Relative relief ratio	**− .849**	.301	.379	.064	− .033	− .110	.124
Gradient ratio	**− .723**	.486	.334	− .242	.177	.002	− .096
Ruggedness number	**.809**	− .085	.259	− .270	.361	.105	− .131
Melton ruggedness number	**− .881**	.192	.357	− .049	.178	.034	− .033
Watershed slope	**− .723**	.486	.334	− .242	.177	.002	− .096
Basin elongation ratio	**.724**	.523	− .319	− .255	− .171	.043	− .041
Hypsometric integral	.517	.224	− .506	− .346	.345	.234	− .309
Asymmetry factor	− .111	.079	.228	.262	**.666**	− .110	.564
Mountain front sinuosity	.206	.248	.373	**− .749**	.085	.255	.243
Basin shape	− .520	**− .744**	.213	− .090	.248	.141	− .161
Valley floor width to height ratio	.564	− .078	.089	− .396	− .084	.471	.314
Eigenvalue	24.116	10.052	6.898	5.566	2.600	2.127	1.727
Explained variance (%)	43.847	18.277	12.543	10.121	4.728	3.867	3.140

Bold numbers represents the strong positive or negative correlation between the parameters
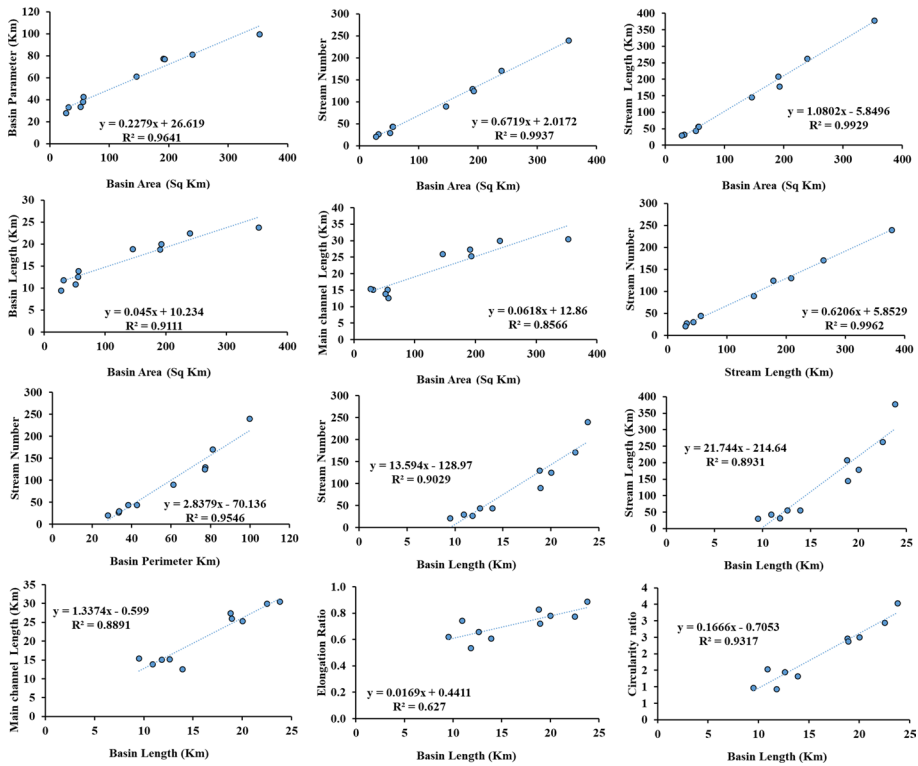
Fig. 5 Cross plot of various morphometric parameters representing their coefficient of determination
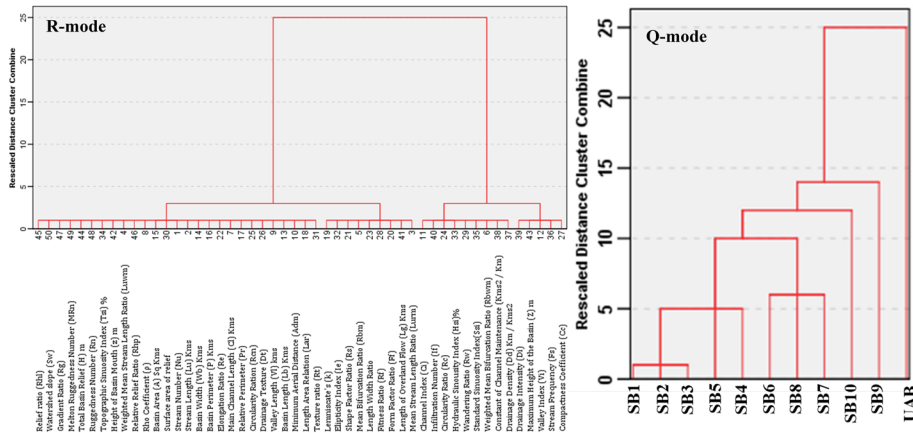
Fig. 6 R-mode and Q-mode, Hierarchal cluster analysis (HCA) of morphometric parameters between UAB and sub-basins

rotation transformation was completed to discover the hidden information from the various constraints. At the end, factor score was considered to find out the most significant factor along with the most influenced sub-basin by each factor (Sajadi et al. 2019).

3.4 Landcover classification

Landuse and landcover (LULC) plays a substantial role in shaping drainage patterns of any basin, it also has a significant role to understand the erosion vulnerability of the basins (Fohrer et al. 2001; Rosenqvist and Birkett 2002; Quilbe et al. 2006; Altaf et al. 2014). The hard rock or non-infiltrating area contributes to increase the surface runoff due to the hindrance to infiltration process (Dams et al. 2013). However, vegetation covers strongly affect the evapo-transpiration, soil moisture and infiltration rate in the basins (Choudhary et al. 1996; Arthur et al.2003; Rashid and Romshoo 2012). The vegetation cover with high amounts of roots plays a significant role in reducing the rates of soil erosion (Carlos et al. 2012; Badar et al. 2013). Similarly, tree canopies and the vegetation cover of minor plants interrupt the precipitation, helping in preventing soil erosion (Mustard and Sunshine 1999; Romshoo et al. 2012).

The Sentinal-2 cloud-free satellite image (October 2018) is obtained from USGS Earth Explorer website and was analysed using pixel-based image analysis (PBIA) method. The PBIA method covers the conventional supervised and unsupervised classification algorithm, where each pixel of the image is allocated a LULC class based on the reflectance value of that pixel (Altaf et al. 2014; Shukla et al. 2020). A total of 120 field-based ground control points (GCPs) and Google Earth images were used for accurate assessment of LULC maps. The landcover (LC) were characterized on the basis of the different classes that were recognized in the study area. The classes generated were vegetation, non-debris cover ice (NDCI), debris cover ice (DCI), water body, snow and rock (Fig. 2e). Table 8 summarizes the statistics of different LC classes of the sub-basins. Based on the response of LC towards erosion, ranking was allocated on the basis of percent area of the classes. Among all the sub-basins, the basin having the highest percentage of the class having direct relation with erosion (e.g. in case of water body, debris and non-debris cover ice and

Table 8 Morphometry and landcover-based watershed prioritization for erosion susceptibility of UAB sub-basins

Sub-basin	Linear parameter					Shape parameter						Relief parameter	Landcover						Cp value	Erosion
	Rbm	Dt	Fs	Dd	Lg	Nu	Rf	Rs	Re	Rc	Cc	H	Vegetation	NDCI	Water	Snow	DCI	Rock		
SB1	3.2	1.7	0.7	1.1	0.7	130.0	0.5	1.9	0.8	0.4	1.6	1.6	0.2	28.1	0.08	7.1	35.3	29.2		
Rank	5	3	7	2	4	8	9	2	9	3	8	1	2	1	6	2	3	4	7.9	High
SB2	3.6	2.4	0.7	1.1	0.7	240.0	0.6	1.6	0.9	0.4	1.5	1.8	0.2	19.3	0.25	5.4	46.1	28.9		
Rank	3	1	6	3	3	10	10	1	10	5	6	6	1	6	1	4	1	3	8.0	High
SB3	3.5	2.1	0.7	1.1	0.7	171.0	0.5	2.1	0.8	0.5	1.5	2.2	8.4	26.5	0.04	4.8	25.4	34.9		
Rank	4	2	5	1	5	9	6	3	7	6	5	7	5	3	8	5	6	8	9.5	High
SB4	4.2	1.5	0.6	1.0	0.5	90.0	0.5	2.5	0.7	0.5	1.4	2.7	28.4	18.7	0.03	7.9	18.3	26.7		
Rank	2	5	9	7	10	6	7	5	6	8	2	8	7	7	10	1	7	2	10.9	Low
SB5	4.6	1.5	0.6	0.9	0.8	125.0	0.5	2.5	0.8	0.5	1.4	3.8	43.8	8.7	0.10	0.8	16.4	30.1		
Rank	1	4	8	8	2	7	8	6	8	9	3	10	9	9	3	9	8	5	11.7	Low
SB6	3.0	1.2	0.8	1.0	0.6	44.0	0.3	2.9	0.7	0.5	1.5	1.8	1.5	21.0	0.09	6.8	36.9	33.6		
Rank	6	6	2	6	7	4	4	7	4	7	4	5	3	5	5	3	2	7	8.7	High
SB7	2.5	0.8	0.9	1.0	0.6	27.0	0.2	4.4	0.5	0.4	1.7	1.7	4.0	26.6	0.03	4.7	29.4	35.3		
Rank	9	6	1	5	9	2	1	7	1	1	10	3	4	2	9	6	5	9	9.7	High
SB8	2.5	1.0	0.8	1.0	0.6	44.0	0.3	3.4	0.6	0.4	1.6	1.7	14.0	21.2	0.05	1.1	30.4	33.2		
Rank	8	7	3	4	8	5	2	9	2	2	9	2	6	4	7	8	4	6	9.6	High
SB9	2.9	0.8	0.8	0.5	0.6	21.0	0.3	3.3	0.6	0.4	1.5	1.8	28.6	17.0	0.10	1.9	15.9	36.5		
Rank	7	9	4	10	6	1	3	8	3	4	7	4	8	8	4	7	9	10	11.2	Low
SB10	2.3	0.9	0.6	0.8	0.9	30.0	0.4	2.3	0.7	0.6	1.3	3.0	78.6	1.1	0.16	0.0	1.0	19.1		
Rank	10	8	10	9	1	3	5	4	5	10	1	9	10	10	2	10	10	1	11.8	Low

Snow) was allotted rank 1, and the lowest percentage of the similar class was allocated as rank 10 (Altaf et al. 2014). Likewise, if any class which is highly confined to erosion (e.g. in case of vegetation and rock cover) was assigned rank 10, and one which has the lowermost percentage of such a class, was assigned rank1.

3.5 Soil erosion and flood hazard zonation

The integrated study of morphometry and landcover (LC) helps to classify the basin (s), which is most vulnerable to erosion (Altaf et al. 2014). Therefore, morphometry and landcover (LC) parameters were evaluated to understand soil erosion susceptibility in the UAB and its sub-basins. For prioritizing soil erosion susceptibility in the study area, the individual rankings of morphometric and LC parameters were averaged for sub-basin to get a common value (Cp) and are calculated as per Altaf et al. (2014) and Javed et al. (2009).

$$\text{Cp} = 1/n \sum_{i=1}^{n} R$$

where Cp: Compound value of a particular basin, R: Rank of a particular basin and n: Number of parameters.

Intensity of soil erosion can be understood by some morphometric parameters having direct relation between them, such as stream frequency, drainage density, drainage texture, mean bifurcation ratio, length of overland flow and basin relief, whereas some of the morphometric parameters have an inverse relation with erodibility such as circulatory ratio, elongation ratio, basin shape, form factor and compactness coefficient (Ratnam et al. 2005). On the basis of direct relating morphometric parameters with erosion rate, the uppermost value of morphometric parameter is allocated with rank 1, and the subsequent successive higher value is allocated rank 2, and vice versa for inverse relating morphometric constraints (Table 8). After allocating ranks to every morphometric constraint, Cp value was obtained by taking the average of ranks allocated to the individual constraints. The sub-basin with the lowermost Cp value is most vulnerable to erosion and needs the highest significance for soil conservation procedures (Altaf et al. 2014).

To understand the degree of flood hazard occurred in the study area we have used the pre-event and post-event photographs of Alaknanda, Khiro Ganga and Laxman Ganga valleys to investigate the major 2013 flood event. Moreover, we utilized the pre-event and post-event, satellite images from Google Earth to evaluate the damage and landscape changes that have been occurred after the disaster (Figs. 9, 10, 11, and 12).

4 Results

The drainages developed in the study area directly depend upon the surface and sub-surface geology, landcover, endogenic and exogenic forces and precipitation of the area (Agarwal and Sharma 2011; Reddy et al. 2004). Keeping in view the above-defined parameters, the entire basin was categories into 10 sub-basins (Fig. 2b) and the morphometric and morphotectonic parameters were analysed.

4.1 Morphometric parameters

The morphometric parameters were categorized into two categories viz. Basin parameters and calculated parameters. The common law of morphometry was followed to calculate the various parameters, as shown in Tables 2 and 3.

4.1.1 Basin parameters

The UAB covers an area of 1527 km^2 having perimeter (P) of 199 km. The area of the sub-basins ranges from 27.3 km^2 (SB9) to 352.3 km^2 (SB2). Likewise, the perimeter for the sub-basins varies from 28 km (SB9) to 99.7 km (SB2). The basin length for UAB is 58.6 km, whereas for sub-basins, it varies from 9.5 km (SB9) to 23.8 km (SB2). UAB comprises of streams up to sixth order, whereas sub-basin SB1, SB2, and SB3 consist of fifth-order streams, SB4, SB5 and SB6 are having streams of fourth order, while SB7, SB8, SB9 and SB10 are having stream up to third order only. The total stream length in the UAB basin is 1536 km, where SB2 comprises of maximum total stream length (378.4 km) and SB9 is having minimum total stream length (30.2 km). UAB basin is having the highest stream length of the first order and as the stream order increases stream length decreases, which is in conformism to the Horton's law of stream number and stream length (Horton 1932; Strahler 1964).

4.1.2 Calculated parameters

The mean stream length ratio (Lurm) of the UAB is 3.1 and for sub-basins it varies between 4.5 (SB4) and 2.3 (SB10). Our results show that the UAB has the Bifurcation ratio (Rb) value between 3.0 and 4.8 (mean: 3.8), while mean bifurcation ratio (Rbm) for the sub-basins ranges between 3.3 (SB1) and 6.2 (SB8). The average Rho coefficient of the UAB is 0.8, while the Rho for the sub-basins ranges from 0.4 (SB8) to 1.2 (SB1).

Under the basin geometry parameter (Table 3), drainage texture (Dt) and elongation ratio (Re) in the sub-basins vary from 0.8 (SB7) to 2.4 (SB2) and 0.6 (SB8, SB9) to 0.9 (SB2), respectively, whereas the stream frequency (Fs) for UAB basin vary between 0.6 (SB4, 5 and 10) to 0.9 (SB7). The wandering ratio (Rw) for the sub-basins varies from 0.9 (SB8) to 1.6 (SB 9) (1.2 for UAB), whereas texture ratio (Rt) ranges between 0.6 (SB9) and 2.7 (SB1). Hydraulic sinuosity index (Hsi) and topographic sinuosity index (Tsi) vary from 57.8 (SB6) to 86.9 (SB1) and 13.1 (SB1) to 42.2 (SB6), respectively.

Under drainage texture class, the stream frequency (Fs) of UAB is 0.7 per km^2, while the Fs for the sub-basins varies from 0.6 (SB4, SB10) to 0.9 (SB7) per km^2. The drainage density (Dd) for UAB is 1.0 and for its sub-basins range between 0.8 (SB10) and 1.1 (SB1, 2 and 3). Similarly, the drainage intensity varies from 0.6 (SB1, 2 and 4) to 1.5 (SB9). The infiltration number (If) varies from 0.4 (SB9) to 0.9 (SB7). SB1 and 2 have the height (3958 m asl) basin mouth height (z), whereas SB10 (1666 m asl) has the lowest basin mouth height. SB2 comprises of the highest peak (7110 m asl) in the basin, whereas SB10 basin highest peak around 5032 m asl. The ruggedness number (Rn) for the UAB varies from 1.2 (SB9) to 4.2 (SB3).

4.2 Morphotectonic parameters

The morphotectonic parameters were analysed for the UAB and its sub-basins by calculating six geomorphic indices (Tables 4 and 5; Figs. 3 and 4). The basin elongation ration (Re) for UAB is 0.75, whereas for the sub-basins it varies between 0.54 and 0.89, indicating slightly tectonically active region. Hypsometric integral (HI) for the 10 sub-basins in UAB shows that all sub-basins range between 0.44 and 0.53, indicating the area is at young to early stage of maturity (Fig. 3). The Asymmetric factor (Af) values in the sub-basins varying from 28.92 to 63.40 (in UAB, Af = 52.17). Among the 10 sub-basins the SB3, SB4, SB7 and SB10 are tilted leftward, while SB1, SB2, SB5, SB6, SB8 and SB9 are tilted rightward from the main channel. The Mountain front sinuosity (Smf) for 10 sub-basins varying from 1.02 to 1.30 with 1.14 for UAB.

Drainage basin shape index (Bs) in sub-basins varied between 1.23 and 2.41 (in SB1 and SB7, respectively) (Table 5). The high values of Bs in SB7 and SB8 ($Bs > 2.3$) referred to the young age and tectonically highly active region, whereas other basins are in the range of tectonically active regions. The calculation for Valley floor width to height ratio (Vf) is carried out for different tributaries and parts of the main channel in UAB. Vf varies between 0.15 and 1.01 for the sub-basins and is calculated about 0.46 for the UAB.

4.3 Statistical analysis

Statistical analysis groups the samples based on the inherent structure and the similarities within the data set. Various statistical studies were performed between different morphometric parameters in sub-basins of UAB. The statistical studies were carried out through applying correlation coefficient analysis, Hierarchal cluster analysis (HCA), and Factor analysis/Principle component analysis (Tables 6 and 7; Figs. 5 and 6).

4.3.1 Correlation coefficient analysis

Correlation coefficient analysis is performed between the morphometric variables in UAB sub-basins (Table 6). On applying correlation coefficient analysis, a strong positive correlation obtained between Basin area and Basin parameter, Stream number, Stream length, Basin length and Main channel length with a correlation coefficient value of 0.96, 0.99, 0.99, 0.91, 0.85, respectively. Similarly, Stream number has a positive correlation between Stream length, Basin perimeter and Basin length with a correlation coefficient of 0.99, 0.95 and 0.90, respectively.

Basin length is also having a positive correlation between stream length, main channel length, elongation ratio and circularity ratio with coefficient of 0.89, 0.89, 0.67 and 0.93, respectively. However, lots of the parameters is having strong negative correlation in between (Table 6; Fig. 5).

4.3.2 Cluster analysis

Hierarchical cluster analysis (HCA) is a statistical technique, which enables the grouping of the UAB sub-basins into different groups according to the morphometric aspects (Fig. 6a, b). Under R-mode HCA analysis (Fig. 6a), there are two major groups, which

are divided further into four different clusters (two clusters each). The first cluster of first group contains stream number, stream length, weighted mean stream length ratio, main channel length, Rho coefficient, valley length, minimum aerial distance, basin length, basin width, basin area, basin perimeter, relative perimeter, length area relation, elongation ratio, circularity ration, drainage texture, surface area of relief, texture ratio, topographic sinuosity index, height of basin mouth, total basin relief, relief ratio, relative relief ratio, gradient ratio, ruggedness number, melton ruggedness number and basin slope, whereas the second cluster covers mean stream length ratio, mean bifurcation ratio, lemniscate's, form factor ratio, shape factor ratio, length width ratio, fitness ratio, ellipticity index, length of overland flow.

Group 2 also contains two clusters. The first cluster contains weighted mean bifurcation ratio, channel index, circularity ratio, wandering ratio, hydraulic sinuosity index, standard sinuosity index, drainage density, constant of channel maintenance, infiltration number, whereas cluster 2 contains valley index, compactness coefficient, stream frequency, drainage intensity, maximum height of the basin.

In Q-mode cluster analysis (Fig. 6b), there are 4 different groups in sub-basins when the rescaled distance of clusters is 5. SB1, 2, 3 and SB4, 5 are in Group 1 and Group 2, respectively, whereas SB6, 7, 8 and SB9, 10 are in Group 3 and 4, respectively.

4.3.3 Principle component analysis (PCA)

On the basis of Principle component analysis (PCA) six factors with eigenvalue > 1 have been accepted to define the principal components (Table 7).

4.3.3.1 Factor/PC1 Factor 1 accounted for 43.9% of total variance and is emphasized as the superior factor in the analysis with the eigenvalue of 24.1. Factor 1 contains stream number, stream length, main channel length, valley length, minimum aerial distance, basin length, basin width, basin area, basin perimeter, relative perimeter, length area relation, lemniscate's, form factor ratio, shape factor ratio, elongation ratio, circularity ration, drainage texture, texture ratio, ellipticity index, basin slope and basin elongation ratio, with high factor loading.

4.3.3.2 Factor/PC2 Factor/PC 2 resembles about 18.3% of total variance with the eigenvalue of 10.1 (Table 7). Factor 2 contains mean bifurcation ratio, channel index, length width ratio, circularity ratio, wandering ratio, sinuosity index, stream frequency, infiltration number and basin shape.

Similarly, factor/PC 3 and 4 accounted 12.5% and 10.1% of total variance with eigenvalue of 5.6 and 2.6, respectively, whereas PC5 and 6 accounted about 3.9% and 3.1% of total variance with eigenvalue of 2.1 and 1.7, respectively.

5 Discussion

Morphometric and morphotectonic analysis, along with statistical technique has been known as a useful tool to understand the hydrological behaviour of the Higher Himalayan regions (Bali et al. 2003). The morphometric-based basin and calculated parameters of the UAB reveal that SB2 is the largest basin with basin area 352 km^2 (basin length 23.8 km), whereas SB9 comprises of the smallest basin having basin area 27.3 km^2 (basin length

9.5 km). The first-order streams were maximum with total cumulative length of 827 km, which reduces as the stream order increases (41 km for sixth-order stream). The sub-basin SB8 shows the highest mean Rb value (6.2), indicating relatively elongated basin. While SB1 shows the lowest mean Rb (3.3). This also indicates that streams up to third order is having steep gradient and rolling through highly dichotomized terrain, due to which high overland flow and less groundwater recharge takes places (Pophare and Balpande 2014). The sub-basins (SB1, 2, 3 and 4) with higher Rho values suggest, better retention of water during flood time which reduces the effect of erosion during heavy discharge (Mesa 2006). The variation in the mean stream length ratio (Lurm) between successive stream orders indicates that UAB and its sub-basins are passing through difference in slope and topographic conditions having a significant correlation with the surface runoff and erosion in the basin (Sreedevi et al. 2005). In the study area, the sub-basins SB6, SB7 SB8 and SB9 having relatively higher stream frequency (Fs) values indicating relatively lower infiltration rate of the bed rock and higher relief in the basins. Sub-basin SB2 and SB3 comprises of drainage texture greater than 2 indicating coarse texture, while all the other sub-basins show very coarse texture (i.e. Dt < 2). The lowest stream frequency (Fs) for the SB4, SB5 and SB10 indicates that basin has high infiltration capacity and hence high vegetation cover (Fig. 2e). Similarly, SB 4, 5, 9 and 10 comprises of low If values, indicating high infiltration and hence less run-off. Low ruggedness number (Rn) SB9 (1.2) indicates that the area is less prone to soil erosion and have intrinsic structural complexity with relief and drainage density.

The assessment of relative tectonic activity in the past has been done by using a number of geomorphic indices (Bull and McFadden 1977; El Hamdouni et al. 2008; Anand and Pradhan 2019). The basin elongation ration (Re) value for the sub-basins varies between 0.6 to 0.9, indicating tectonically active region (Table 4). Moreover, Re in SB2 is close to 1.0 indicating regions of very low relief, whereas other basins Re value ranges between 0.6 and 0.8 indicates that the area is associated with high relief and steep ground slope (Strahler 1964). The Hypsometric curve (HC) and Hypsometric integral (HI) for the UAB and its sub-basins shows that the area is young to early stage of maturity (Fig. 3). In the mature stage, hydrologic response of the sub-basin shows slow rate of erosion (Ritter et al. 2002) until very high runoff peaks occur due to flood event. In the study area, SB4 and SB5 have suffered a heavy flood events in the recent past with the outlet having wider valleys and broader flood plain representing higher rate of erosion. High potential for flooding in the basin is also due to the higher average drainage slope leading to faster movement of surface runoff with higher velocity through the basin outlet and thus broadening of the flood plains (Singh et al. 2008). The higher value of basin shape (Bs) (SB7 and SB8; > 2.3) indicates the primarily down-cutting in areas having continuous rapid uplift within the basins (Ramírez-Herrera 1998; Sajadi et al. 2019). The valley floor width to height ratio (Vf) values indicates that a large portion of the basin area have relatively active mountain fronts and are experiencing rapid uplift, suggesting recent tectonic movements. The Vf values also indicate that the sub-basins are mostly V-shaped and that streams are cutting downward or eroding horizontally into contiguous hill slopes. The observed triangular facets in the study area with the help of Landsat and Google earth image, also conforms the presence of recent tectonic activities happening in the study area (Fig. 7).

The results obtained from Hierarchal cluster analysis is same as obtained from correlation coefficient analysis and PCA indicating significant correlation among morphometric parameters in study basin (Figs. 5, 6 and Tables 6, 7). HCA for sub-basins according to morphometric parameters (Fig. 7) classify sub-basins into four different clusters. SB4 and SB5 come in a same group, indicating high correlation in-between, which is also
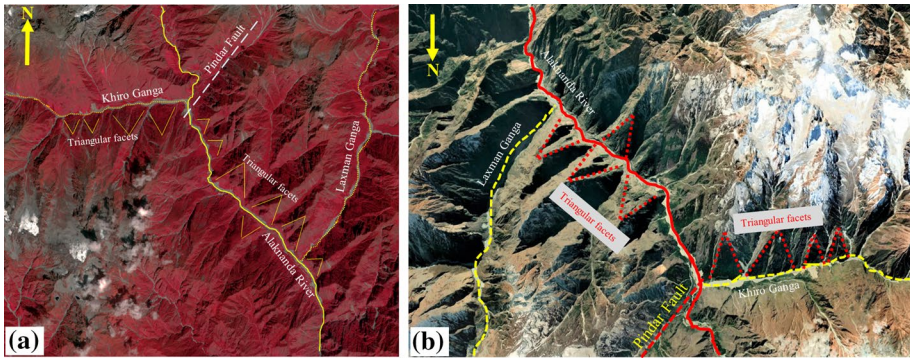
Fig. 7 **a** Landsat and **b** Google earth image (Maxer Technologies, Image Landsat/Copernicus dated 06 Mar 2014), with marked triangular facets in the study area. (Note: Flow direction of the Alaknanda river is from North to South)

conformed from morphotectonic analysis. Similarly, SB1, SB2 and SB3 comes in a single group and SB6, SB7 and SB8 comes in another group. The cluster analysis of sub-basins revels the similarity between sub-basins falling in a single group which is also been observed during field visits. PCA analysis also reveals that all the Factor 1 parameters are same which fall under cluster 1 of HCA, indicating high correlation of the data sets, and hence it is considered as a most influential factor.

5.1 Determination of relative degrees of flood hazard

The degree of flood hazard for individual sub-basin was examined on the basis of El Shamy's model (El Shamy1992). A relation between bifurcation ratio vs. drainage density, and stream frequency vs. bifurcation ratio was used to determine the degree of hazard in UAB sub-basins (Fig. 8a, b). According to El Shamy's model flood hazard map is classified into three different zones: A, B, and C. The zone (A) high flash floods potentiality zone, zone (B) moderate potential for floods and (C) have less flood potential. Figure 8, shows that all the sub-basins lies on zone (A) having high degree of flash flood possibilities in the study area.
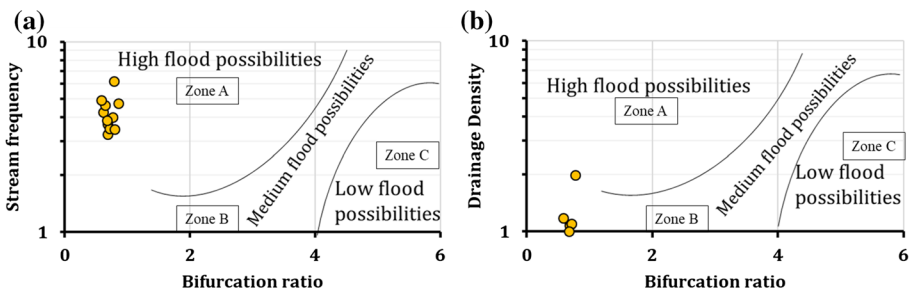
Fig. 8 Cross plot between **a** Stream frequency vs. bifurcation ratio and **b** drainage density vs. bifurcation ratio, indicating flash flood possibilities using some hydro-morphometric parameters based on El Shamy's model (El Shamy 1992) in UAB and its sub-basins
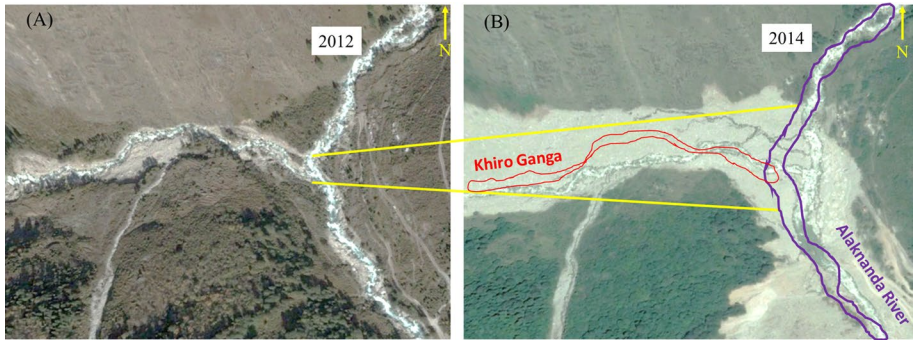
Fig. 9 Google Earth Image of Khiro Ganga river **a** before and **b** after major flood event of June 2013. Red and violet line representing Khiro Ganga and Alaknanda river profile before the flood event, whereas yellow line represents the change on the span of the confluence sight. Both the google earth image are from Maxer Technologies, Image Landsat/Copernicus, dated **a** 11 Sept 2012 and **b** 06 Mar 2014

5.2 Case study of a major flood event

In UAB, Khiro Ganga (SB4) river meets Alaknanda river at Benakuli and has devastating effect caused by the flash flood during June 2013 flood event. Benakuli village is near to Badrinath temple in UAB, having sharp changes in the geomorphology of the study area. The Khiro Ganga river travels through wide valley having loose unconsolidated glacial moraine and colluvial deposits with good vegetation cover (Mehta et al. 2016). As per the Iat classification and presence of triangular facets, SB4 sub-basin also comes under highly tectonically active region (Table 5, Fig. 7). The Khiro valley is having thick forest of Deodar, Oak, Birch and meadows in the higher reaches of the region. According to local peoples, heavy rainfall during June 15–17th, 2013 huge landslides was occurred all over the valley causing due to toe cutting by the high flood in the river. Local peoples also told that the valley was having huge number of springs with high discharge all over the year. When the discharge of the river due to flood was high, it brought and deposited enormous amount of debris, boulders and big trees which resulted blocking the main Alaknanda river. During the flood event, there were huge number of tree trunks deteriorating river water quality in the form unusual odour (kind of rotten smell from river water) all over the valley. Figure 9 and 10, shows the spam of the Khiro Ganga changes from 63 m to 196 m at the confluence sight and pushed the main flowing Alaknanda river toward left bank by depositing huge amount of debris at the confluence sight. The El Shamy's model shows that UAB is highly flood-prone zone, but erosion classification shows SB4 sub-basin (Khiro Ganga basin) is comparatively highly resistive to erosion (Fig. 8). The most prominent reason behind less susceptibility to erosion of SB4 basin is due to high vegetation cover and low drainage density and hence huge amount of stored groundwater.

At the downstream of the Benakuli village, flood water destroyed and completely filled the 14 m high 400-megawatt J.P. Vishnuprayag Hydro-Electric Dam site with huge debris (Fig. 11). The effect of the flood was so much devastating that it changed the Alaknanda river spam from 49 m to 194 m, at upstream of the dam. The small town of Lambaghar (downstream of the Dam) was entirely washed away and no proof of settlement was left (Mehta et al. 2016). The high flood possibility in this region bellow
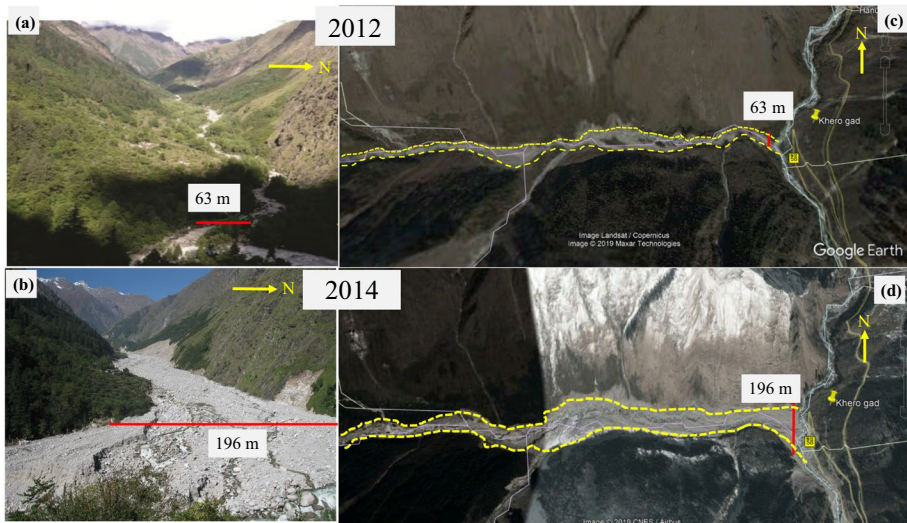
Fig. 10 Photographs of Khairo Ganga during **a** 2012 and **b** 2014 along with Google Earth image of **c** 2012 and **d** 2014 showing huge landslide in the Khiro Ganga on 16 June 2013. After the cloud burst event river brought enormous debris and destroyed the vegetation cover in the valley. (Photograph **a** from Mehta et al. 2016). Both the google earth image are from Maxer Technologies, Image Landsat/Copernicus, dated **c** 11 Sept 2012 and **d** 06 Mar 2014
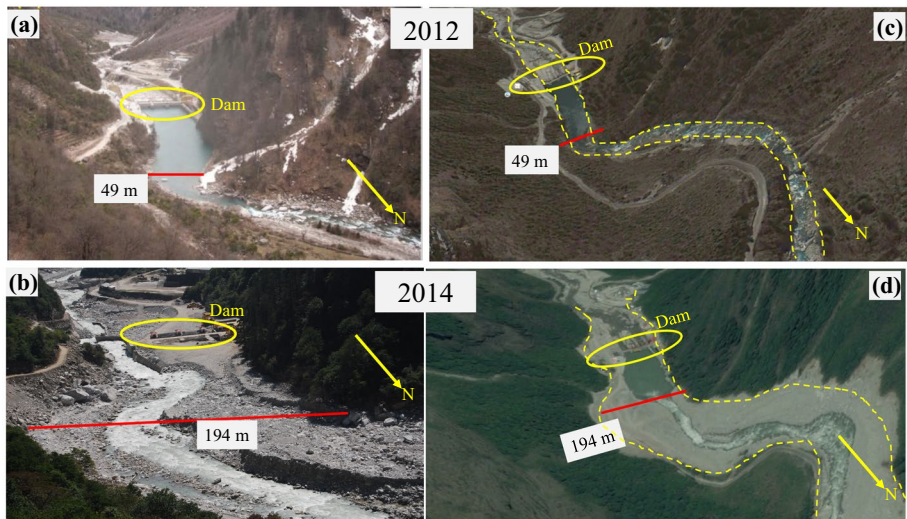

Fig. 11 Photographs of Alaknanda river during **a** 2012 and **b** 2014 along with Google Earth image of **c** 2012 and **d** 2014 showing huge debris cover (~ 20 m) before JP 400-megawatt Vishnuprayag Hydro-Electric Project on 16 June 2013. [Photograph **a** from Mehta et al. (2016)]. Google earth image is from **c** Maxer Technologies, Image Landsat/Copernicus, dated 11 Sept 2012 and **d** CNES/Airbus, Landsat/Copernicus dated 06 Mar 2014

Benakuli in compression to Badrinath basin is the low valley floor to valley height ratio and high bifurcation ratio.

A similar kind of flood event was observed in Pulna village (SB5), situated 5 km upstream from the Govind Ghat on the right bank of the Laxman Ganga. During the disaster, flooded Laxman Ganga dumped a huge amount of sediment in Pulna village and the village was totally suppressed under thick debris cover (Mehta et al. 2016) (Fig. 12b, c). Pulna village is established at, respectively, wide valley in the SB5 sub-basin having high basin relief, indicating tectonically highly active and susceptible to flood events (Table 5).

5.3 Sub-basins susceptibility to tectonic activity and soil erosion

On the basis of Relative Tectonic Activity Index (Iat) (Table 5, Fig. 13a), UAB is classified under tectonically active region. SB1, SB4, SB6, SB7, SB8 and SB9 (60% area) are very highly tectonically active, while the sub-basin SB2 and SB5 are high tectonically active. SB10 and SB3 are moderately and the lowest tectonically active region, respectively. Thus, almost 80% of the UAB comes under high tectonically active region. The different geomorphic expressions such as offsetting of stream courses, presence of landslide cones and presence of triangular fault facets are indicator of faulting and hence clearly indicates that the study area is undergoing differential tectonic activity (Fig. 7).
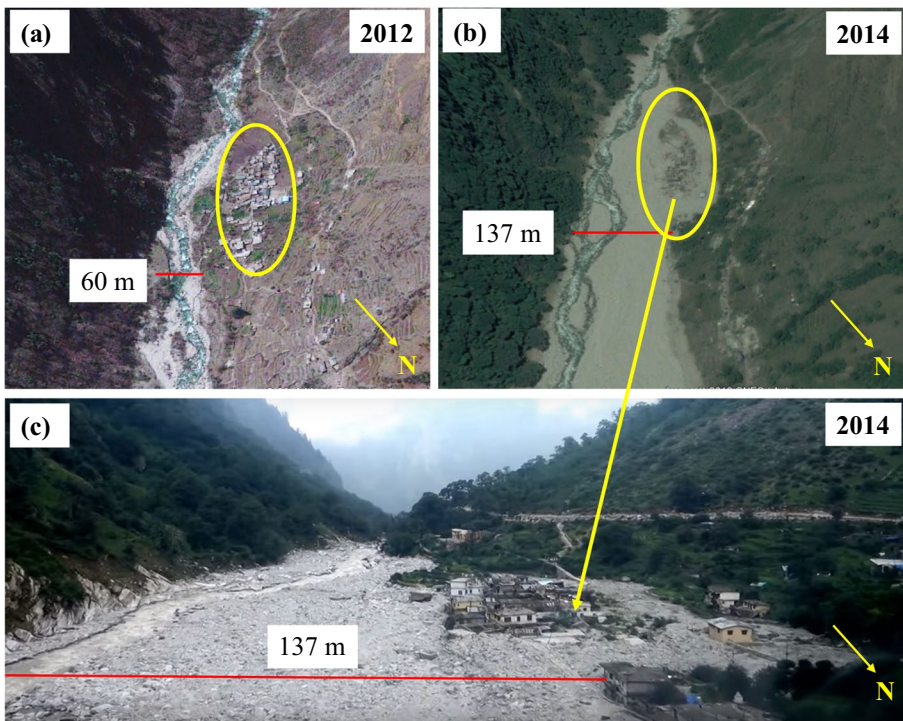
Fig. 12 Google Earth image of Laxaman Ganga river near Pulna village during **a** 2012 and **b** 2014 along with **c** photograph during 2014 taken through Helicopter ride, showing huge debris cover after the major flood event on 16 June 2013. Google earth image is from **a** CNES/Airbus, Landsat/Copernicus dated 27 March 2012 and **b** Maxer Technologies, Image Landsat/Copernicus dated 06 March 2014
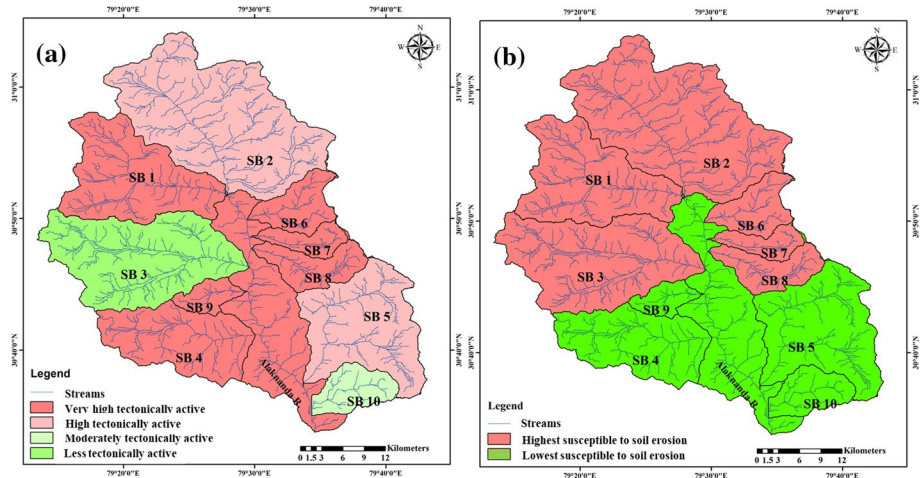
Fig. 13 Map representing **a** degree of tectonic activity and **b** susceptible to soil erosion, in sub-basins of Upper Alaknanda river basin

The combined morphometric and LC results were analysed, which show that the priority order of sub-basins for erosion rate is SB1 > SB2 > SB6 > SB3 > SB8 > SB7 > SB4 > SB 9 > SB5 > SB10 (Table 5). Figure 13b represents the sub-basins susceptible to soil erosion. UAB basin SB4, SB5, SB9 and SB10 are the lowest susceptible to soil erosion, whereas other sub-basins are characterized as highly susceptible to soil erosion (Table 8). Thus, almost 60% of the area comes under highly vulnerable to soil erosion (Fig. 13b).

6 Conclusion

In the present study we have tried to evaluate the role of morphometry and morphotectonic on drainage behaviour in Upper Alaknanda river basin on the basis of remote sensing, GIS, and statistical analysis tool. Fifty morphometric and six morphotectonic parameters were calculated to understand the tectonic setting of the UAB basin. The morphometric analysis showed that first-order stream in all the sub-basins is having maximum stream length and the highest-order stream is having minimum stream length. Bifurcation ratio and stream frequency shows that streams up to third order is having steep gradient and rolling through highly dichotomized terrain, due to which high overland flow and less groundwater recharge takes places, whereas drainage density clearly indicates the high flood possibility in the region. Morphotectonic parameters indicates relatively young to early mature geological stage of sub-basins and tectonically active region. Drainage basin asymmetry factor indicates 40% of the area underlined the leftward tilting and 30% of the area underlined the rightward tilt in sub-basins, whereas rest 30% lies under stable environmental setting. The UAB is having comparatively high relief and is linked with minor/major thrust faults and triangular facets that indicate tectonic activity, ultimately having significant role in the basin hydrology. Statistical modelling (HCA and factor analysis) were used to identify the most significant constraints over these ten sub-basins. HCA shows that SB4 and SB5 comes in a same group and are having high flood possibilities. PCA analysis with the help of varimax transformation derive seven principal factors with eigenvalue greater

than 1. The factor 1 accounts for 43.9% of the total variance, whereas factor 2 accounts for 18.3% of the total variance. The combination of morphometric analysis with landcover of the area determines that about 60% of the area is highly susceptible to soil erosion. However, flood hazard degree assessment using El Shamy's model indicates high flood possibility in all the sub-basins. The relative tectonic analysis shows that about 80% of the area is under high tectonically active zone. SB1, SB4, SB6, SB7, SB8 and SB9 are very high tectonically active regions, whereas SB2 and SB5 are high tectonically active while, SB10 and SB3 are moderately and the lowest tectonically active region, respectively. The three case studies of major flood event during June 2013 in the basin support the results obtained from morphometric and morphotectonic analysis.

Overall, this study will help in ranking the basins and decision making for captivating soil and water conservation procedures that are susceptible for integrated watershed management in highly critical and important zone. However, accessibility to the higher region is not possible due to adverse climatic and logistical conditions, hence a more detail work is required with more field-based investigations and surveys to understand the hydrology of region in more detail.

Author contribution RKD, SPR and NP designed and coordinated this study. NP, AB, PS, and SM conducted the field data collection. AB conducted morphometric and morphotectonic analysis on Arc GIS software under the guidance of SM, PS, NP. NP wrote the paper with important contribution from PS, RKD, SPR, SM and AB.

Compliance with ethical standards

References

Agarwal K, Sharma V (2011) Quaternary tilt-block tectonics in parts of Eastern Kumaun Himalaya, India. Zeitschrift für Geomorphologie 55(2):197–208

Ahmad T, Harris N, Bickle M, Chapman H, Bunbury J, Prince C (2000) Isotopic constraints on the structural relationships between the lesser Himalayan series and the high Himalayan crystalline series, Garhwal Himalaya. Geol Soc Am Bull 112(3):467–477

Altaf S, Meraj G, Romshoo SA (2014) Morphometry and land cover based multi-criteria analysis for assessing the soil erosion susceptibility of the western Himalayan watershed. Environ Monit Assess 186(12):8391–8412

Anand AK, Pradhan SP (2019) Assessment of active tectonics from geomorphic indices and morphometric parameters in part of Ganga basin. J Mt Sci 16(8):1943–1961

Arthur W, Bennett W, Edens P, Bell S (2003) Effectiveness of training in organizations: a meta-analysis of design and evaluation features. J Appl Psychol 88(2):234–245

Astras T, Soulankellis N (1992) Contribution of digital image analysis techniques on Landsat-5 TM imageries for drainage delineation. A case study from the Olympus mountain, west Macedonia, Greece. In: Proceedings of the 18th annual conference of remote sensing society, University of Dundee, Dundee, Scotland, pp 15–17

Badar B, Romshoo S, Khan M (2013) Integrating biophysical and socioeconomic information for prioritizing watersheds in a Kashmir Himalayan lake: a remote sensing and GIS approach. Environ Monit Assess 185(8):6419–6445

Bali R, Awasthi DD, Tiwari NK (2003) Neotectonic control on the geomorphic evolution of the Gangotri Glacier Valley, Garhwal Himalaya. Gondwana Res 6(4):829–838

Bali R, Agarwal KK, Ali SN, Rastogi SK, Krishna K (2012) Drainage morphometry of Himalayan Glacio-fluvial basin, India: hydrologic and neotectonic implications. Environ Earth Sci 66(4):1163–1174

Bishop M (2002) Geomorphic change in high mountains: a western Himalayan perspective. Glob Planet Change 32(4):311–329

Bull WB (1977) Tectonic geomorphology north and south of the Garlock fault, California. In: Geomorphology in arid regions, proceeding 8th annual geomorphology symposium, State University New York at Binghamton, 1997, pp 115–137

Bull WB, McFadden LD (1977) Tectonic geomorphology north and south of the Garlock Fault, California. In: Doehring DO (ed) Proceedings of the eighth annual geomorphology symposium of geomorphology in arid regions, State University of New York, Binghamton, pp 115–138

Cannon PJ (1976) Generation of explicit parameters for a quantitative geomorphic study of Mill Creek drainage basin. Oklahoma Geol Notes 36(1):3–16

Carlos GH, Ramon JB, Artemio C, de Luisa M (2012) A regional analysis of the effects of largest events on soil erosion. CATENA 95:85–90

Choudhary MA, Lal R, Guo P (1996) Tillage effects on nonpoint source pollution. In: Proceedings of the conference on engineering in agriculture and food processing Gatton College, The University of Queensland, 24–27 November, vol 25(3)

Clarke JI (1966) Morphometry from maps. In: Dury GH (ed) Essays in geomorphology. Elsevier, New York, pp 235–274

Cox RT (1994) Analysis of drainage-basin symmetry as a rapid technique to identify areas of possible quaternary tilt-block tectonics: an example from the Mississippi Embayment. Geol Soc Am Bull 106(5):571–581

Dams J, Dujardina J, Reggersa R, Bashira I, Cantersb F, Batelaana O (2013) Mapping impervious surface change from remote sensing for hydrological modelling. J Hydrol 485:84–95

Demoulin A (2011) Basin and river profile morphometry: a new index with a high potential for relative dating of tectonic uplift. Geomorphology 126(1–2):97–107

Diakakis M (2011) A method for flood hazard mapping based on basin morphometry: application in two catchments in Greece. Nat Hazards 56(3):803–814

El Hamdouni R, Irigaray C, Fernández T, Chacón J, Keller EA (2008) Assessment of relative active tectonics, southwest border of the Sierra Nevada (southern Spain). Geomorphology 96(1–2):150–173

El Shamy IZ (1992) Recent recharge and flash flooding opportunities in the Eastern Desert, Egypt. Ann Geol Surv Egypt, XVIII, pp 323–334

Faniran A (1968) The index of drainage intensity—a provisional new drainage factor. Aust J Sci 31:328–330

Fohrer N, Haverkamp S, Eckhardt K, Frede HG (2001) Hydrologic response to land use changes on the catchment scale. Phys Chem Earth (B) 26:577–582

Granato D, Putnik P, Kovačević DB, Santos JS, Calado V et al (2018) Trends in chemometrics: food authentication, microbiology, and effects of processing. Compr Rev Food Sci Food Saf 17(3):663–677

Gravelius H (1914) Grundrifi der gesamten gewcisserkunde, Band I: Flufikunde [Compendium of Hydrology, vol. I. Rivers, in German]. Goschen, Berlin

Hare PW, Gardner TW (1985) Geomorphic indicators of vertical neotectonism along converging plate margins, Nicoya Peninsula, Costa Rica. Tecton Geomorphol 4:75–104

Horton RE (1932) Drainage-basin characteristics. EOS Trans Am Geophys Union 13(1):350–361

Horton RE (1940) An approach towards the physical interpretation of infiltration-capacity. Soil Sci Soc Am Proc 5:399–417

Horton RE (1945) Erosional development of streams and their drainage basins; hydrophysical approach to quantitative morphology. Geol Soc Am Bull 56(3):275–370

Howard AD (1990) Role of hypsometry and planform in basin hydrologic response. Hydrol Process 4(4):373–385

Ifabiyi IP, Eniolorunda NB, Dangulla M, Rufai K (2012) Correlates of domestic water demand in Sokoto metropolis, Sokoto State, Nigeria. J Sci Res Rev 1(5):069–077

Jain SK, Kumar S, Varghese J (2001) Estimation of soil erosion for a Himalayan watershed using GIS technique. Water Resour Manag 15:41–54

Javed A, Khanday MY, Ahmed R (2009) Prioritization of sub-watersheds based on morphometric and land use analysis using remote sensing and GIS techniques. J Indian Soc Remote Sens 37(2):261

Joshi V, Kumar K (2006) Extreme rainfall events and associated natural hazards in Alaknanda valley, Indian Himalayan region. J Mt Sci 3(3):228–236

Kaiser HF (1960) The application of electronic computers to factor analysis. Educ Psychol Meas 20(1):141–151

Keller EA, Pinter N (2002) Active tectonics: earthquakes, uplift, and landscape. Prentice Hall, New Jersey

Lee I, Yang J (2009) Common clustering algorithms (chapter 313). In: Brown SD, Tauler R, Walczak B (eds) Comprehensive chemometrics, vol 2. Elsevier, Amsterdam, pp 557–618

Lin A, Ren Z, Jia D, Wu X (2009) Co-seismic thrusting rupture and slip distribution produced by the 2008 Mw 7.9 Wenchuan earthquake, China. Tectonophysics 471(3–4):203–215

Lyew-Ayee P, Viles H, Tucker G (2007) The use of GIS-based digital morphometric techniques in the study of cockpit karst. Earth Surf Proc Land 32(2):165–179

Maeda EE, Heiskanen J, Thijs KW, Pellikka PK (2014) Season-dependence of remote sensing indicators of tree species diversity. Remote Sens Lett 5(5):404–412

Mayer L (1986) Tectonic geomorphology of escarpments and mountain fronts. In: Wallace (ed) Studies in geophysics. National Academy, Washington, DC, pp 125–135

Mehta M, Dobhal DP, Shukla T, Gupta AK (2016) Instability processes triggered by heavy rain in the Garhwal Region, Uttarakhand, India. In: Climate change, glacier response, and vegetation dynamics in the Himalaya. Springer, pp 219–234

Melton MA (1957) An analysis of the relations among elements of climate, surface properties and geomorphology. Columbia University, Office of Naval Research Project NR 389-042, Technical Report 11. New York: Columbia University

Melton MA (1958) Correlation structure of morphometric properties of drainage systems and their controlling agents. J Geol 66(4):442–460

Mesa LM (2006) Morphometric analysis of a subtropical Andean basin (Tucuman, Argentina). Environ Geol 50(8):1235–1242

Miller VC (1953) A quantitative geomorphic study of drainage basin characteristics in the Clinch Mountain Area, Virginia and Tennessee. Department of Geology Columbia University, New York, pp 389–402

Morisawa ME (1962) Quantitative geomorphology of some watersheds in the Appalachian Plateau. Geol Soc Am Bull 73(9):1025–1046

Mustard JF, Sunshine JM (1999) Spectral analysis for earth science: investigations using remote sensing data. Remote Sens Earth Sci Man Remote Sens 3:251–307

Nag SK, Chakraborty S (2003) Influence of rock types and structures in the development of drainage network in hard rock area. J Indian Soc Remote Sens 31(1):25–35

Pallard B, Castellarin A, Montanari A (2009) A look at the links between drainage density and flood statistics. Hydrol Earth Syst Sci 13(7):1019–1029

Pareta K, Pareta U (2011) Quantitative morphometric analysis of a watershed of Yamuna basin, India using ASTER (DEM) data and GIS. Int J Geom Geosci 2(1):248–269

Patton PC, Baker VR (1976) Morphometry and floods in small drainage basins subject to diverse hydrogeomorphic controls. Water Resour Res 12(5):941–952

Pérez-Peña JV, Azor A, Azañón JM, Keller EA (2010) Active tectonics in the Sierra Nevada (Betic Cordillera, SE Spain): insights from geomorphic indexes and drainage pattern analysis. Geomorphology 119(1–2):74–87

Pfeffer WT, Arendt AA, Bliss A, Bolch T, Cogley et al (2014) The Randolph Glacier Inventory: a globally complete inventory of glaciers. J Glaciol 60(221):537–552

Pike RJ, Wilson SE (1971) Elevation-relief ratio, hypsometric integral, and geomorphic area-altitude analysis. Geol Soc Am Bull 82(4):1079–1084

Pophare AM, Balpande US (2014) Morphometric analysis of Suketi river basin, Himachal Himalaya, India. J Earth Syst Sci 123(7):1501–1515

Quilbe R, Rousseau AN, Duchemin M, Poulin A et al (2006) Selecting a calculation method to estimate sediment and nutrient loads in streams: application to the Beaurivage River (Quebec, Canada). J Hydrol 326:295–310

Ramírez-Herrera MT (1998) Geomorphic assessment of active tectonics in the Acambay Graben, Mexican volcanic belt. Earth surface processes and landforms. J Br Geomorphol Gr 23(4):317–332

Rana N, Singh S, Sundriyal YP, Rawat GS, Juyal N (2016) Interpreting the geomorphometric indices for neotectonic implications: an example of Alaknanda valley, Garhwal Himalaya, India. J Earth Syst Sci 125(4):841–854

Rashid I, Romshoo SA (2012) Impact of anthropogenic activities on water quality of Lidder River in Kashmir Himalayas. Environ Monit Assess 185:4705–4719

Ratnam KN, Srivastava YK, Rao VV, Amminedu E, Murthy KSR (2005) Check dam positioning by prioritization of micro-watersheds using SYI model and morphometric analysis—remote sensing and GIS perspective. J Indian Soc Remote Sens 33(1):25

Reddy GPO, Maji AK, Gajbhiye KS (2004) Drainage morphometry and its influence on landform characteristics in a basaltic terrain, Central India—a remote sensing and GIS approach. Int J Appl Earth Obs Geoinf 6(1):1–16

Ritter D, Kochel R, Miller J (2002) Process geomorphology. Mc Graw-Hill, New York

Romshoo SA, Bhat SA, Rashid I (2012) Geoinformatics for assessing the morphometric control on hydrological response at watershed scale in the Upper Indus Basin. J Earth Syst Sci 121(3):659–686

Rosenqvist A, Birkett CM (2002) Evaluation of JERS −1 SAR mosaics for hydrological applications in the Congo river basin. Int J Remote Sens 23(7):1283–1302

Sajadi P, Singh A, Mukherjee S, Luo P, Chapi K, Salari M (2019) Multivariate statistical analysis of relationship between tectonic activity and drainage behavior in Qorveh–Dehgolan basin Kurdistan, Iran. Geocarto Int. https://doi.org/10.1080/10106049.2019.1611948

Sarangi A, Bhattacharya AK (2000) Use of geomorphological parameters for sediment yield prediction from watersheds. J Soil Water Conserv 44:99–106

Schumm SA (1956) Evolution of drainage systems and slopes in badlands at Perth Amboy, New Jersey. Geol Soc Am Bull 67(5):597–646

Schumm SA (1963) Sinuosity of alluvial rivers on the Great Plains. Geol Soc Am Bull 74(9):1089–1100

Sharma R, Sahai B, Karale RL (1985) Identification of erosion-prone areas in a part of the Ukai catchment. In: Proceedings, sixth Asian conference on remote sensing. Hyderabad. National Remote Sensing Agency, pp 121–126

Shukla DP, Dubey CS, Ningreichon AS et al (2014) GIS-based morpho-tectonic studies of Alaknanda river basin: a precursor for hazard zonation. Nat Hazards 71(3):1433–1452

Shukla AK, Ojha CSP, Garg RD, Shukla S, Pal L (2020) Influence of spatial urbanization on hydrological components of the Upper Ganga River Basin, India. J Hazard Toxic Radioact Waste 24(4):04020028

Singh AK, Hasnain SI (1998) Major ion chemistry and weathering control in a high-altitude basin: Alaknanda River, Garhwal Himalaya, India. Hydrol Sci J 43(6):825–843

Singh O, Sarangi A, Sharma MC (2008) Hypsometric integral estimation methods and its relevance on erosion status of north-western lesser Himalayan watersheds. Water Resour Manag 22(11):1545–1560

Smith KG (1950) Standards for grading texture of erosional topography. Am J Sci 248(9):655–668

Sreedevi PD, Subrahmanyam K, Ahmed S (2005) Integrated approach for delineating potential zones to explore for groundwater in the Pageru River basin, Cuddapah District, Andhra Pradesh, India. Hydrogeol J 13(3):534–543

Strahler AN (1950) Davis' concepts of slope development viewed in the light of recent quantitative investigations. Ann Assoc Am Geogr 40(3):209–213

Strahler AN (1952a) Dynamic basis of geomorphology. Geol Soc Am Bull 63(9):923–938

Strahler AN (1952b) Hypsometric (area-altitude) analysis of erosional topography. Geol Soc Am Bull 63(11):1117–1142

Strahler AN (1964) Part II. Quantitative geomorphology of drainage basins and channel networks. Handbook of applied hydrology. McGraw-Hill, New York, pp 4–39

Thompson JR, Taylor MP, Fryirs KA, Brierley GJ (2001) A geomorphological frame work for river characterization and habitat assessment. Aquat Conserv Mar Freshw Ecosyst 11:373–389

Valdiya KS (1987) Trans-Himadri Thrust and domal upwarps immediately south of collision zone and tectonic implications. Curr Sci 56:200–209

Valdiya KS (1999a) Tectonic and lithological characterization of Himadri (Great Himalaya) between Kali and Yamuna rivers, central Himalaya. Him Geol 20(2):1–17

Valdiya KS (1999b) Rising Himalaya: advent and intensification. Curr Sci 76(4):514–524

Vega M, Pardo R, Barrado E, Debán L (1998) Assessment of seasonal and polluting effects on the quality of river water by exploratory data analysis. Water Res 32:3581–3592

Vijith H, Satheesh R (2006) GIS based morphometric analysis of two major upland sub-watersheds of Meenachil river in Kerala. J Indian Soc Remote Sens 34(2):181–185

Wakode HB, Dutta D, Desai VR, Baier K, Azzam R (2013) Morphometric analysis of the upper catchment of Kosi River using GIS techniques. Arab J Geosci 6(2):395–408

Walker F, Allen MB (2012) Offset rivers, drainage spacing and the record of strike-slip faulting: The Kuh Banan Fault, Iran. Tectonophysics 530–531:251–263

Williams PW, McDougall I, Powell JM (1972) Aspects of the quaternary geology of the Tari-Koroba area, Papua. J Geol Soc Aust 18(4):333–347

Yan B, Lin A (2015) Systematic deflection and offset of the Yangtze River drainage system along the strike-slip Ganzi-Yushu-Xianshuihe Fault Zone, Tibetan Plateau. J Geodyn 87:13–25

Affiliations

Neeraj Pant[1] [ORCID] **· Rajendra Kumar Dubey[1] · Anand Bhatt[2] · Shive Prakash Rai[3] · Prabhat Semwal[2] · Sumit Mishra[2]**

Neeraj Pant
pant.neeraj007@gmail.com

[1]   Department of Applied Geology, IIT (ISM) Dhanbad, Dhanbad, India

[2]   Department of Geology, Hemvati Nandan Bahuguna, Garhwal University, Srinagar, Garhwal, India

[3]   Centre of Advanced Study in Geology, Institute of Science, Banaras Hindu University, Varanasi, India